

1 Global changes in extreme temperature indices from
2 daily climate model data

S. Russo,¹ A. Sterl,¹

S. Russo, Royal Netherlands Meteorological Institute (KNMI), P.O. Box 201, NL-3730 AE De Bilt, Netherlands (russo@knmi.nl).

A. Sterl, Royal Netherlands Meteorological Institute (KNMI), P.O. Box 201, NL-3730 AE De Bilt, Netherlands (sterl@knmi.nl).

¹Royal Netherlands Meteorological
Institute (KNMI), NL-3730 AE De Bilt,
Netherlands.

Abstract. Climate change indices derived from model daily extreme temperature data are computed and analyzed to study the change of climatic extremes between 1950 and 2100. We use data from the ESSENCE project, in which a 17-member ensemble simulation of climate change in response to the SRES A1b scenario has been carried out using the ECHAM5/MPI-OM climate model. The large size of the dataset gives the opportunity to accurately detect the change of extreme climate indicators. We choose extreme temperature indices from the Expert Team on Climate Change Detection, Monitoring and Indices (ETCCDMI), focusing on percentile based and duration indices. Additionally, we define some new indices measuring the intensity of daily temperature extremes. To study extremes within different subsequent 50-year time intervals (1950-2000, 2001-2050 and 2051-2100) we use corresponding reference periods (respectively 1961-1990, 2011-2040, and 2061-2090). Trends of the indices within each of the three 50-year periods are estimated using the Mann-Kendall slope estimator. The trends found in our model data for the period 1950-2000 compare well with those reported in the literature from observations. Future trend patterns resemble those from the 1950-2000 period, but have larger amplitudes. Thus the pattern of extreme temperature change is already emerging from the weather noise. Outside the tropics, the trend of indices defined from minimum daily temperatures is greater in absolute value than the trend of indicators related to maximum daily temperatures. The trend of the annual temperature range ($T_{\max} - T_{\min}$) is positive or close to zero over the tropics and negative over the ex-

26 tratropics, indicating that the value of the yearly maximum temperature is
27 increasing faster than the minimum in the tropics and *vice versa* in the ex-
28 tratropics. Finally, using a class of frequency curves defined by Johnson (John-
29 son, 1949), we study index probability density functions (PDF) for eight re-
30 gions. All PDFs shift in the direction of warming.

1. Introduction

31 Future climate change is generally believed to lead to an increase in climate variability
32 and in the frequency, intensity and duration of extreme events. The definition of an
33 extreme is not simple if we want to define an extreme coherently over the entire Globe.
34 In the last few years many indices have been developed by different authors to compare
35 climate change between different regions. The utility of an index is to monitor climate
36 and estimate when climate change will happen. They measure intensity, frequency and
37 duration of temperature and precipitation events. An index represents events that occur
38 several time per season or year, giving it more robust statistical properties than measures
39 of extremes which are so far in the tail of the distribution that they are not observed every
40 year.

41 *Frich et al.* [2002] (henceforth FEA02) produced a global dataset of derived indicators
42 to clarify whether frequency and severity of climatic extremes changed during the sec-
43 ond half of the 20th century. They found that the number of days for which the daily
44 minimum temperature is above the 90th percentile has increased for most of the land
45 area, with a reduction of frost days and increasing in growing season length. *Kiktev et*
46 *al.* [2003] generally confirmed these results with more robust statistical methods. The
47 joint World Meteorological Organization Commission for Climatology (CCI)/World Cli-
48 mate Research Programme (WCRP) project on Climate Variability and Predictability
49 (CLIVAR) Expert Team on Climate Change Detection, Monitoring and Indices (ETC-
50 CDMI) coordinated two complimentary efforts to enable the global analysis of extremes
51 (see <http://ccma.seos.uvic.ca/ETCCDMI> for details). One effort was the international

52 coordination of the development of a suite of climate change indices which primarily focus
53 on extremes. The second ETCCDMI effort was to coordinate regional workshops with
54 the aim of addressing gaps in data availability and analysis in previous global studies
55 [e.g., *Frich et al.*, 2002]. *Alexander et al.* [2006] (henceforth AEA06) applied the suite of
56 climate indices developed by ETCCDMI to a data set with good coverage. They studied
57 the empirical probability density function (PDF) of the calculated indices and found that
58 over 70% of the sampled land area has a significant decrease in the annual occurrence of
59 cold nights (TN10p index) and a corresponding increase in warm nights (TN90p index).

60 In this paper we use modelled daily temperature data for the period 1950-2100 to
61 calculate some of the temperature indices formulated by FEA02 and reviewed later by
62 the ETCCDMI. Most of the indices that were used in the past are related to the estimation
63 of duration or occurrence of extreme events, without any consideration of their intensity.
64 We therefore also define some indices that measure the intensity of extreme events. This
65 study is a complement to the paper of *Sterl et al.* [2008], who used the same model data
66 to investigate the change of the temperature to be expected only once in 100 years. In
67 the present paper we focus on much milder extremes, which makes it possible to better
68 compare the model results with observations.

69 We divide the period 1950-2100 into three consecutive non-overlapping 50-year periods.
70 The findings for the first period (1950-2000) are in agreement with previous studies [e.g.,
71 *Jones et al.*, 1999], regional studies using daily data [e.g., *Yan et al.*, 2002], and with the
72 results of AEA06. We focus on extremes in the future periods by moving the threshold
73 from the 1961-1990 reference period (FEA02 definition) to reference periods 2011-2040 and
74 2061-2090 and calculate the indices with respect to these reference periods. Additionally,

75 we also calculate them for the whole period (1950-2100) using the threshold of the first
76 period. This gives us the opportunity to distinguish changes caused by a shift of the PDFs
77 from changes caused by an increased variability. We focus on the temporal variability of
78 the indices by using non-parametric trend analysis within the three 50-year intervals.
79 Finally, we consider eight sub-regions of the Globe where we study the PDFs of the
80 indices by fitting with Johnson's method of translation [*Johnson, 1949*].

2. Essence project and model data

81 In the ESSENCE project (Ensemble SimulationS of Extreme weather events under
82 Nonlinear Climate changE) a 17-member ensemble of runs with a state-of-the-art climate
83 model was performed to investigate the range of possible future climate change (*Sterl et*
84 *al.*, [2008]). The model used is the ECHAM5/MPI-OM coupled climate model developed
85 at the Max-Planck-Institute for Meteorology in Hamburg. Model runs start in 1950 and
86 end in 2100. For the historical part (1950-2000) the concentrations of greenhouse gases
87 (GHG) and tropospheric sulfate aerosols are specified from observations, while for the
88 future part (2001-2100) they follow the SRES A1b scenario [*Nakicenovic et al.*, 2000].
89 The runs are initialized from a long run in which historical GHG concentrations have
90 been used until 1950. Different ensemble members are generated by disturbing the initial
91 state of the atmosphere. Gaussian noise with an amplitude of 0.1 K is added to the initial
92 temperature field. The initial ocean state is not perturbed. For more information about
93 the model see *Sterl et al.* [2008].

3. Index selection and definition

94 All indices used in this work are derived from daily maximum and minimum tempera-
 95 tures. AEA06 have divided the indices into 5 different classes: percentile based indices,
 96 duration indices, absolute indices, threshold indices and other indices. In addition to
 97 indices from the first two classes we use the Extreme Temperature Range index (ETR;
 98 classified as “other index”) and some newly defined indices that allow us to study changes
 99 in the intensity of warm and cold days. Their definition is given below.

100 **Percentile based indices:** These are indices with the threshold defined by using a
 101 percentile of an empirical PDF. Percentile based indices taken from the ETCCDMI and
 102 used in this study are given in Table 1. As an example, we discuss one of them, TX90p,
 103 which is given by

104 TX90p (Occurrence of warm days): Percent (or number) of days per month (or year)
 105 with maximum daily temperature over the 90th percentile for the 1961-1990 reference
 106 period.

107 The daily threshold for the reference period 1961-1990 is defined as the n-th (in this case
 108 n=90) percentile, centered on a 5-day window (calculated using the method of Appendix D
 109 of *Zhang and Yang* [2004]). For example, for a fixed day d the threshold is the n-th
 110 percentile of the set of data A_d defined as

$$A_d = \bigcup_{y=1961}^{1990} \bigcup_{d'=d-2}^{d'+2} T_{y,d'}. \quad (1)$$

111 Different reference periods are used to focus on future extremes. The time period studied
 112 (1950-2100) is split into three consecutive 50-year periods, with the reference periods for
 113 the second and the third period being 2011-2040 and 2061-2090, respectively. In addition
 114 to calculating the indices for these three different reference periods we also calculate them

115 for the whole period 1950-2100 by using the threshold from the first reference period
116 (1961-1990).

117 There are at least two reasons to shift the reference period: the first is that by moving the
118 threshold we are eliminating the effect of the mean shift of the distribution when focusing
119 on future extremes. By also calculating the indices with respect to the first period we
120 just include this effect. The second is that the indices counting the number of days over
121 the 10th percentile (occurrence of cold days, cold spell duration index, etc.) tend to have
122 too many zero values in the future if we fix 1961-1990 as the reference period. After year
123 2000 most of the data move above the 10th percentile, making the index meaningless.

124 For the same reason we define a new TN10p index by calculating it for the whole
125 period using the threshold from the last reference period (2061-2090). We call this index
126 TN10p-ft, where “ft” indicates future threshold.

127 To test whether the highest extremes show a different behaviour than the relative mod-
128 erate 90th percentiles, we also investigated indices based on the 95th and 98th percentiles.
129 As we found no difference between the trends from these three sets of indices, the results
130 related to the indices based on the higher percentiles are not shown.

131 **Duration indices:** Duration indices are defined as the time period in which the data
132 are above some threshold. Warm Spell Duration Index (WSDI) and Cold Spell Duration
133 Index (CSDI) are two examples of temperature duration indices. Their definitions are
134 given in Table 1. As before, different reference periods are used to calculate WSDI and
135 CSDI within the three 50-year periods considered.

136 **Other Indices:** The intra-annual extreme temperature range (ETR) is defined as
137 the difference between yearly maximum and minimum temperature (see Table 1). It

138 spans the most extreme high-temperature events of the summer season and the most
 139 extreme low temperature events of the winter season. If the yearly minimum temperature
 140 increases faster (slower) than the yearly maximum temperature the sum of scale and shape
 141 parameters of the temperature distribution is decreasing (increasing), while changes in the
 142 location parameters are not important. Thus changes in ETR are only related to changes
 143 in the tails of the temperature distribution.

144 **Intensity of occurrence of warm and cold nights and days** (ITX90p, ITN90p,
 145 ITX10p, ITN10p): The previous percentile based indices represent an empirical way to
 146 study the change of the number of days over a threshold. However, they do not give
 147 any information about the *values* above that threshold. It could be that the number of
 148 threshold exceedances is increasing while the values over the threshold have no significant
 149 trend or *vice versa*. To estimate this effect we introduce the intensity indices. They are
 150 defined in analogy to the “degree-days” used to characterize the coldness of a winter or
 151 the hotness of a summer by summarizing the differences between the daily temperature
 152 and the daily threshold over a year. The threshold is taken from the percentile-based
 153 indices. For example, ITX90p is defined as

$$ITX90p = \sum_{i=1}^{365} \Delta T_i, \tag{2}$$

154 where

$$\Delta T_i = \begin{cases} T_i - Thr_i & \text{if } (T_i - Thr_i) \begin{cases} > 0 \\ < 0 \end{cases} \end{cases} . \tag{3}$$

155 Here T_i is the daily maximum temperature of day i within a year, and Thr_i is the
156 threshold for the same day.

157 A physical interpretation of a trend in ITX90p is obtained by dividing the trend values
158 by 36.5 (10% of days in a year), which approximately represents the number of days over
159 the 90th percentile threshold. For example, let the trend be 12 degree-days per decade.
160 Dividing by 36.5 days gives 0.32 degrees/decade, meaning that for a constant number of
161 days above the threshold (10% of the days in a year) each of these days is warming by
162 0.32 K per 10 years.

4. Data analysis methods

163 To quantify global climate variability we use two different approaches: trend analysis
164 and the study of the PDF of the indices.

4.1. Trend analysis

165 Index data do not necessarily have a Gaussian distribution, so a simple linear least
166 square estimation is not sufficient to detect a trend. To overcome this problem we use
167 the Mann-Kendall non-parametric slope estimator, which does not assume a distribution
168 for the residuals [*Sen*, 1968]. Its definition is detailed in Appendix A of *Wang and Swail*
169 [2001]. When investigating trends we have to pay attention to the autocorrelation of the
170 data. If a trend test is applied to serially correlated data (which is usually the case for
171 climatological time series) the trend detection results are not reliable. In the case of the
172 Mann-Kendall estimator the test may reject the null hypothesis of no trend (H_0) more
173 often than specified by the significance level [*von Storch*, 1995; *Zhang and Zwiers*, 2004].
174 We therefore use the procedure proposed by *Zhang et al.* [2000] and apply the test after

175 pre-whitening the time series [von Storch, 1995; Zhang and Zwiers, 2004]. Details about
 176 the method are well explained by Wang and Swail [2001] (Appendix A).

177 The trend is estimated for each of the seventeen samples individually. As the distribu-
 178 tion of the slopes is normal due to the independence of the 17 samples, the final trend is
 179 the mean of the 17 slopes. To calculate the significance level of the final trend we consider
 180 the Kendall S statistic, which estimates whether our data are concordant or discordant.
 181 The S-values for each sample (S_i) are summed to form the overall statistic S_k ,

$$S_k = \sum_{i=1}^{17} S_i. \quad (4)$$

182 The distribution of S_k can be approximated by a normal distribution with expectation
 183 equal to the sum of the expectations of the individual S_i under the null hypothesis (zero
 184 here), and variance equal to the sum of their variances. S_k is standardized by subtracting
 185 its expectation $\mu_{S_k} = 0$ and dividing by its standard deviation σ_{S_k} ,

$$Z_{S_k} = \begin{cases} \frac{S_k-1}{\sigma_{S_k}} & \text{if } S_k \begin{cases} > 0 \\ = 0 \\ < 0 \end{cases} \end{cases}, \quad (5)$$

186 where $\sigma_{S_k} = \sqrt{\sum_{i=1}^{17} \sigma_i}$, with $\sigma_i = (n_i/18)(n_i - 1)(2n_i + 5)$ being the variance of the
 187 individual slope estimates, and n_i is the number of data in the i-th sample. The null
 188 hypothesis (no trend) is rejected at significance level α if $|Z_{S_k}| > Z_{crit}$, where Z_{crit} is the
 189 value of the standard normal distribution with a probability of exceedence of $\alpha/2$.

4.2. Fitting by using Johnson's frequency curves

190 We use Johnson's fit [Johnson, 1949] to calculate probability density functions for eight
 191 different regions. We use the same regions that were selected by Chauvin et al. [2007]

192 because of their homogeneous response. Four of them are situated in the latitude band
 193 40°S-40°N, and four are outside of this band (see Table 2 and upper left panel of Figure 1).
 194 Indices are averaged over these regions and then fitted by using Johnson's frequency curves
 195 [*Johnson, 1949*]. The Johnson system is a flexible system to describe statistical distribu-
 196 tions. It translates the general distribution function of a continuous random variable x ,
 197 whose distribution is not known, to a normal distribution,

$$Z = \gamma + \delta \cdot g\left(\frac{x - \xi}{\lambda}\right), \quad (6)$$

198 where Z is the normal standard variate with zero mean and unit variance.

By setting

$$y = \frac{x - \xi}{\lambda} \quad (7)$$

199 equation (6) is simplified to

$$Z = \gamma + \delta \cdot g(y), \quad (8)$$

200 where $g(y)$ is one of the following functions:

1) $g(y) = y$	Normal	
2) $g(y) = \log(y)$	Log - Normal	
3) $g(y) = \log\left(\frac{y}{1-y}\right)$	Unbounded	(9)
4) $g(y) = \log(y + \sqrt{y^2 + 1})$	Bounded	

201 The Johnson system classifies sample distributions according to these four families of
 202 frequency curves.

203 The probability density function of y is given by

$$p(y) = \gamma + \delta \cdot g'(y) \cdot p(Z) = \frac{\delta}{\sqrt{2\pi}} g'(y) \cdot \exp\left(\frac{-1}{2[\gamma + \delta \cdot g(y)]^2}\right). \quad (10)$$

204 The linear relationship (7) implies that the distribution of x has the same shape as that
 205 of y . By definition, the standard deviation of x is λ times that of y , and ξ represents a
 206 simple translation that only affects the expected values of the x distribution. Accordingly,
 207 λ and ξ in equation (6) are simply scale and location parameters, respectively, while γ and
 208 δ determine the shape of the distribution (10). We estimate the Johnson parameters from
 209 quantiles, using the procedure of *Wheeler* [1980]. Alternatively, they can be estimated
 210 from the moments [*Hill and Holder*, 1976].

4.3. Fitting GEV

211 To study the change in yearly maxima and minima we use the generalized extreme value
 212 (GEV) distribution. GEV fitting is used to confirm our results related to changes of the
 213 ETR index, in order to have robust results. According to the extremal types theorem
 214 [*Coles*, 2001] the GEV provides a model for the distribution of block maxima. The data
 215 are divided into blocks of equal length, and the GEV is fit to the set of block maxima.
 216 The fit is done by using the Maximum-Likelihood fitting implemented in the R package
 217 *ismev* (<http://cran.r-project.org/web/packages/ismev/index.html>). The likelihood ratio
 218 test is used to check whether the two-parameter Gumbel model is a plausible reduction
 219 of the GEV, which has three parameters. For the test the deviance statistic is calculated
 220 and compared with the χ^2 distribution.

5. Trend Results

5.1. General considerations

221 The data are split into three consecutive periods of 50 years, representing respectively
222 past (1950-2000), (near-)present (2001-2050) and future (2051-2100). The results are
223 related to the extreme values within each of the periods. As explained in section 3
224 each of the periods has its own reference period (1961-1990, 2011-2040, and 2061-2090,
225 respectively) to define the percentiles. In this way we are sure that the indices are not
226 affected by the shift of the mean and that we are really focusing on the extremes.

5.2. Past - comparison with observed data

227 To assess the degree to which our model is able to reproduce observed trends in extreme
228 indices, we first compare our results with those of AEA06. They used a global daily
229 observed dataset to calculate the extreme indices. In Figures 1-5 we show trends of the
230 indices for the three periods defined above. We start the discussion of these figures by
231 comparing their upper panels (period 1950-2000) with the results of AEA06.

5.2.1. Occurrence of cold nights and days

232 Figure 1 shows the decadal trends of the occurrences of cold nights, TN10p (left),
233 and cold days, TX10p (right). The figure does not contain white points as the trend is
234 significant at the 5% confidence level everywhere and for all periods studied.
235

236 The trends of TN10p and TX10p (Figure 1, upper panels) are negative everywhere,
237 indicating a decrease of the number of cold days and nights. Their magnitude falls in the
238 same range as those derived from the observations. For example, the trend for the occur-
239 rence of cold nights over Eurasia and South Africa varies between -6 and -3 days/decade,
240 which is in very good agreement with AEA06. On the other hand, the trends over South
241 America are only -3 days/decade, which is less than observed (up to -6 days/decade).

242 The highest trend of TN10p (> 6 days/decade) is found over Africa. Unfortunately, this
243 value cannot be compared with observations due to the lack of data.

244 For cold days (TX10p) AEA06 found significant trends only over 46% of the area for
245 which they had data. This area comprises South Africa, Alaska and parts of Asia, where
246 the trend values range between -6 and 0 days/decade. In the same regions our calcu-
247 lated trend for TX10p is a smaller, with values ranging between -3 and 0 days/decade.
248 Only small regions show higher values. The highest trends are again found over Africa,
249 where they cannot be compared with observations. Over parts of the US the observations
250 indicate a non-significant positive trend which is not confirmed by the model.

251 **5.2.2. Occurrence of warm nights and days**

252 For TN90p and TX90p (upper panels of Figure 2) our trend results show good agreement
253 with those of AEA06. Over North America both trends are around 3 days/decade in both
254 model and observations. Over Eurasia the modelled trend of TN90p is lower than the
255 observed one, but for TX90p both sources give trends of the same magnitude of around
256 3 days/decade. Modelled trends in the data-void tropical and subtropical regions are
257 much higher than in the extratropics, exceeding 9 days/decade in the Congo basin.

258 **5.2.3. Intensity of cold nights and warm days**

259 The intensities of cold nights (ITN10p) and warm days (ITX90p) show the same overall
260 development as do the numbers of these days. The intensity of the cold nights decreases
261 (Figure 3, upper left) and that of the warm days increases (Figure 3, upper right).

262 For both indices the magnitude of the trend is smallest in the tropical belt, most no-
263 ticeably in the northern part of South America. The magnitude of both trends increases
264 towards the poles. However, this increase is much larger for the cold nights than for the

265 warm days. While the former reaches values of more than -10 K/decade in Siberia and
266 Canada, the maximum of the latter is only 7 K/decade. In short, cold nights warm much
267 faster than warm days.

268 **5.2.4. Cold and Warm Spell Duration Indices**

269 Over the period 1950-2000 the length of the warm spells (Figure 4, upper left) signif-
270 icantly increases everywhere, while the length of the cold spells (Figure 4, upper right)
271 exhibits positive trends over North America, but both positive and negative trends over
272 Eurasia. Similar results were obtained by AEA06, who also find positive trends in CSDI
273 over North America. Due to our large ensemble our trends in both indices are statistically
274 significant nearly everywhere, but they are generally smaller than those of AEA06 which,
275 however, are significant in limited areas only.

276 **5.2.5. ETR index**

277 Both FEA02 and AEA06 have found a decreasing trend in the yearly temperature
278 range from observed data covering the extratropics and a small part of the subtropics.
279 Our model data show comparable trends (Figure 5, upper left). The modelled ETR index
280 shows a significant negative trend with magnitude between -0.1 and -0.5 K/decade over
281 Canada, Alaska and some small areas in Eurasia. On the other hand we find an increase in
282 ETR in some parts of the tropical regions of America. Unfortunately, this finding cannot
283 be compared to observations. For both observational and modelled data trends in ETR
284 are significant only in a small fraction of the land area.

285 **5.2.6. Conclusion**

286 In conclusion our model does a reasonable job in reproducing observed trends in the
287 analyzed extreme temperature indices. While the patterns of the trends compare well,

288 the magnitudes are generally lower. However, due to the much larger dataset (17 runs)
289 our results are statistically more robust. Furthermore, we have data also in those regions
290 (mainly tropics) for which enough observational data do not exist. We therefore feel
291 encouraged to use the model data to assess projected changes in the extreme indices.

5.3. Future extremes

292 5.3.1. Occurrence of cold nights and days

293 Both indices continue to decrease in the future (Figure 1, middle and lower panels),
294 albeit with an increasing speed. For both future periods the patterns of the trends are
295 very similar, but values tend to be higher for the future period than they are for the
296 near-present one, and much higher than for the past. As for the present period the largest
297 trends are found over the tropical regions, where the trend of TN10p reaches values around
298 -20 days/decade in the Congo basin, and trends are generally higher for the cold nights
299 than for the cold days.

300 5.3.2. Occurrence of warm nights and days

301 The number of both warm nights and warm days keeps increasing (Figure 2, middle
302 and lower panels). For both indices the patterns are very similar in all three periods, but
303 the magnitudes are much higher in the near-present and future periods than in the past
304 period. Both indices show the highest trends in the tropics, where maxima reach values of
305 more than 20 days/decade, and lowest values at higher latitudes. Generally the trends
306 are higher for the warm nights (TN90p) than they are for the warm days (TX90p).

307 Comparing the trends of the “cold” indices (TN10p and TX10p) with those of the
308 “warm” ones (TN90p and TX90p) we see that they have similar patterns. Absolute values
309 are highest in the tropics and smallest at high latitudes. However, at high latitudes the

310 numbers of cold days and nights decrease faster than those of warm days and nights
311 increase, while the opposite is true in the tropics. We can anticipate that this leads to
312 opposite trends in ETR, the yearly temperature range. It will probably decrease at high
313 latitudes and increase at lower latitudes.

314 **5.3.3. Intensity of cold nights and warm days**

315 The trend patterns of the intensity indices for cold nights (ITN10p) and warm days
316 (ITX90p) (Figure 3) are similar for all three periods, but as for the occurrence indices
317 their magnitudes are higher for the near-present and future periods than they are for the
318 past one.

319 A comparison between the intensity indices and their occurrence counterparts shows an
320 interesting difference. For both occurrence indices the magnitude of the trends is larger in
321 the tropical areas than it is at high latitudes (left panels of Figures 1 and 2). The patterns
322 for the corresponding intensity indices (Figure 3) are exactly opposite with largest trends
323 at high latitudes and smallest in the tropics. Clearly, the temperature increase at high
324 latitudes is much larger than near the Equator [see also *Brown et al.*, 2008] and outweighs
325 the increase in the number of days above the threshold in the tropics. Relatively few days
326 with high exceedance values (high latitudes) contribute stronger to the intensity indices
327 than does a large number of days with small exceedences (tropics).

328 **5.3.4. Cold and warm spell duration indices**

329 The trends of both duration indices are quite similar for all three periods investigated
330 (Figure 4). The duration of warm spells (WSDI) increases everywhere with highest values
331 being reached in a latitude belt around 20°N. The magnitude of the trend in the duration
332 of cold spells (CSDI) is generally larger than that for WSDI. Interestingly, the length

333 of cold spells is projected to increase in some parts of America as well as in southern
334 Australia. In all these areas both the occurrence and the intensity of cold nights decreases
335 (left panels of Figures 1 and 3). An increase of CSDI thus means that cold spells will
336 become longer, but less severe.

337 **5.3.5. Extreme Temperature Range index (ETR)**

338 The area with significant trends of the ETR index increases in the near-present and
339 future periods (Figure 5). Strong negative trends of up to -1 K/decade are found poleward
340 of 40° , while a slight increase is found equatorward of this latitude. This behaviour is in
341 accordance with that of the intensity indices (Figure 3). The decrease of ITN90p is much
342 larger than the increase of ITX90p over the higher latitudes, but smaller in the tropics.

6. Mean shift and extremes

6.1. Method

343 In this section we calculate the probability density functions of TX90p, TN10p-ft, and
344 ETR and examine their change over time. As we do not know the generic form of the
345 PDFs of the indices beforehand, we use Johnson's method (section 4.2) to estimate their
346 forms. The error of the fits is estimated by using bootstrapping with 10.000 repetitions.
347 For all fits the error ranges between 3% and 10%.

348 The data are split into six periods of 25 years. This is short enough to consider them
349 stationary and at the same time to have enough data for a reliable fit. Furthermore,
350 other studies have got PDFs using the same time periods (FEA02, AEA06). Spatially,
351 we consider the average of the indices over the eight regions defined in Table 2. They are
352 chosen to represent different climates with independent means.

6.2. Cold nights and warm days: Mean shift

353 Figures 6 and 7 show the PDFs of the occurrence of warm days (TX90p, based on
354 reference period 1961-1990) and cold nights (TN10p-ft, i.e., based on reference period
355 2061-2090) for the six 25-year periods. For both indices and all regions the PDFs show
356 significant changes over time. The PDF of TX90p moves from left to right, indicating
357 warming. The PDF of TN10p-ft moves in the opposite direction. As TN10p-ft is computed
358 with respect to the threshold of the last period (2061-2090), this also indicates warming.
359 Generally, the shape and kurtosis parameters do not show significant changes over time.
360 Exceptions are northern South America (Figures 6f and 7f) and Australia (Figures 6g
361 and 7g), where the shape parameters change from positive to negative values. The reason
362 is that in these areas the upper tail of the PDFs reaches the possible maximum (365),
363 making a long right tail impossible. Location and scale parameters increase everywhere,
364 meaning that warming is taking place in all regions, and that the variability of the indices
365 increases, so that and the extremes are increasing faster than the mean.

366 Figure 8 shows the location parameters of the PDFs for each region. The numbers on
367 the x-axis denote the six 25-year periods. The index values on the y-axis are expressed
368 in percent of days in a year and represent the change between the location parameter for
369 the given 25-year period and that of the first period (1951-1975). The black circles and
370 gray crosses correspond to TX90p and TN10p-ft, respectively. The shift of both indices
371 towards a warmer climate is obvious.

372 The difference of the location parameters between the last and the first period gives
373 an estimate of the total shift of the two indices over the whole 150 years. It is shown in
374 Figure 8i, where grey and black histograms correspond to TN10p-ft and TX90p, respec-

375 tively. Confirming earlier results, this figure shows that over mid to high latitudes the
 376 location parameter of TN10p-ft changes more than that of TX90p: cold temperatures are
 377 increasing faster than warm temperatures. Equatorward of about 40° there are regions
 378 like Australia or the US where the location parameter of TX90p is changing as fast as
 379 or even faster than that of T10p-ft. In northern South America, the region of maximum
 380 shift (Figure 8i), the number of warm days (by the standards of 1961-1990) reaches 227
 381 (62%) by the end of the century, while by the standards of the last period (2061-2090)
 382 there are 281 (77%) cold nights during the period 1950-1975.

6.3. Cold nights and warm days: Extremes

383 Changes in extremes, here the occurrence of cold nights and warm days, can have two
 384 reasons: a shift of the mean temperature, and a change of the scale and shape of the
 385 temperature PDF, i.e., an increased variability. The frequency distribution of a climate
 386 parameter for a given period and area varies around a mean value. An extreme event
 387 is defined by a deviation from the mean with a low frequency of occurrence [*Dankers*
 388 *et al.*, 2008]. As shape and kurtosis of the PDFs do not change much (section 6.2),
 389 changes of temperature extremes are due to a shift (location parameter) and widening
 390 (scale parameter) of the distribution.

391 To estimate the relative importance of changes in both parameters we define the quantity

$$\Delta E_i = \Delta\mu_i + 2\Delta\sigma_i. \quad (11)$$

392 For TX90p $\Delta\mu_i$ and $\Delta\sigma_i$ are the differences between period i (where $i = 2, 3, 4, 5, 6$
 393 numbers the 25-year periods) and the first period of the location and scale parameter,

394 respectively. For TN10p-ft $i = 1, 2, 3, 4, 5$, and $\Delta\mu_i$ and $\Delta\sigma_i$ are calculated with respect to
395 the last period. ΔE_i represents the change in the extremes as the sum of the shift ($\Delta\mu_i$)
396 and increased variability ($\Delta\sigma_i$). The factor 2 indicates that we are focusing on the 98th
397 percentile of the calculated PDF. If the variability increases ($\Delta\sigma_i$ positive) the extremes
398 change more than the mean shift of the distribution ($\Delta\mu_i$) suggests.

399 The red circles and crosses in Figure 8 represent the changes of the extremes of TX90p
400 and TN10p-ft, respectively, as estimated by ΔE_i . We see that in the future the extremes
401 are increasing more than the mean in nearly all regions. The extra increase due to the
402 increasing variability reaches up to 15%. The only region where changed variability has
403 no influence on the extremes is northern South America, where the shift is very strong
404 and where we have detected large changes of the shape parameter (section 6.2).

6.4. Extreme temperature range

405 Figure 9 shows the changing PDFs for the extreme temperature range (ETR). The
406 values on the x-axis are Kelvin and estimate the difference between yearly peaks of max-
407 imum and minimum daily temperature. As a further confirmation of the previous results
408 we see that over the extratropical areas the curves are shifting from the right to the left,
409 indicating a decrease of the temperature range. In this areas, cold temperatures rise faster
410 than warm temperatures. Over the latitude band between 40°S and 40°N the difference
411 between annual maximum and minimum temperatures increases as warm temperatures
412 rise faster than cold temperatures.

7. Conclusions

413 In this paper we have investigated projected changes of some frequently used indices
414 describing extreme temperature events, such as the occurrence of cold nights or warm
415 days. We do so by using data from the ESSENCE project [Sterl *et al.*, 2008], in which a
416 17-member ensemble of runs with a comprehensive climate model for the period 1950-2100
417 under the SRES A1b emission scenario was performed.

418 For the period 1950-2000 we find a good correspondence between our model results
419 and those derived from observations [Alexander *et al.*, 2006]. Patterns of modelled trends
420 in the extreme indices are qualitatively equal to those derived from observations, and in
421 many cases there is even quantitative agreement.

422 For the future the modelled trend patterns resemble those of the historical period (1950-
423 2000), but the change is faster. Taken together with the close resemblance of observed
424 and modelled trend patterns over the historical period this means that the patterns of
425 extreme temperature changes are already emerging from the weather noise.

426 The temperature increase at high latitudes is much larger than near the Equator and
427 outweighs the increase in the number of days above the threshold in the tropics. Relatively
428 few days with high exceedance values (high latitudes) contribute stronger to the intensity
429 indices than does a large number of days with small exceedances (tropics).

430 The increase of indices describing extreme temperatures is caused by a combination of
431 changes in the mean temperature and an increase of the variability. The increase of the
432 variability accounts for an extra increase of the extremes of up to 15% above that caused
433 by the mean shift.

434 In extratropical areas indices describing *cold* extremes rise faster than those describing
435 *warm* ones, leading to a reduction of the extreme temperature range index, the difference

436 between the yearly maximum and minimum temperatures. In the tropics the development
437 is opposite, with *warm* indices increasing faster than *cold* ones.

438 **Acknowledgments.** This work was funded by the EU (contract no. MRTN-CT-2005-
439 019374) as part of the SEAMOCS research training network. The ESSENCE project,
440 led by Wilco Hazeleger (KNMI) and Henk Dijkstra (UU/IMAU), was carried out with
441 support of DEISA, HLRS, SARA and NCF (through NCF projects NRG-2006.06, CAVE-
442 06-023 and SG-06-267). We thank the DEISA Consortium (co-funded by the EU, FP6
443 projects 508830 / 031513) for support within the DEISA Extreme Computing Initiative
444 (www.deisa.org). The authors thank Camiel Severijns (KNMI) and HLRS and SARA
445 staff for technical support.

References

- 446 Alexander L.V, X. Zhang, T. C. Peterson, J. Caesar, B. Gleason, A. M. G. Klein Tank,
447 M. Haylock, D. Collins, B. Trewin, F. Rahimzadeh, A. Tagipour, K. Rupa Kumar,
448 J. Revadekar, G. Griffiths, L. Vincent, D. B. Stephenson, J. Burn, E. Aguilar, M.
449 Brunet, M. Taylor, M. New, P. Zhai, M. Rusticucci, and J. L. Vazquez-Aguirre (2006),
450 Global observed changes in daily climate extremes of temperature and precipitation, *J.*
451 *Geophys. Res.*, *113*, D05109, doi:10.1029/2006JD008091.
- 452 Brown, S.J, J. Ceasar, and C.A.T. Ferro, (2008), Global changes in extreme daily tem-
453 perature since 1950, *J. Geophys. Res.*, *113*, D05109, doi:10.1029/2006JD008091.
- 454 Chauvin, F., and S. Denvil (2007), Changes in severe indices as simulated by two French
455 coupled global climate models, *Global Planet. Change*, *57*, 96 - 11.

- 456 Coles, S. (2001), An introduction to statistical modeling of extreme values, *Springer*,
457 *London. 208 pp.*
- 458 Dankers R., and R. Hiederer (2008), Extreme Temperatures and Precipitation in
459 Europe: Analysis of a High-Resolution Climate Change Scenario, *JRC Scientific*
460 *and Technical Reports*, [http://eusoils.jrc.ec.europa.eu/ESDB_Archive/eusoils_docs/-](http://eusoils.jrc.ec.europa.eu/ESDB_Archive/eusoils_docs/Images/EUR_23291.PDF)
461 [Images/EUR_23291.PDF](http://eusoils.jrc.ec.europa.eu/ESDB_Archive/eusoils_docs/Images/EUR_23291.PDF).
- 462 Frich, P., L. V. Alexander, P. Della-Marta, B. Gleason, M. Haylock, A. M.G. Klein Tank,
463 and T. Peterson (2002), Observed coherent changes in climatic extremes during the
464 second half of the twentieth century, *Clim.Res.*, *19*, D05109, 193 - 212.
- 465 Hill, I.D., R. Hill, and R.L. Holder (1976), Fitting Johnson curves by moments, *Applied*
466 *Statistics*, *25*, No. 2, 180-189.
- 467 Johnson, N.L., (1949), System of frequency curves generated by methods of translation,
468 *Biometrika*, *36*, 149 - 176.
- 469 Jones, P. D., M. New, D. E. Parker, S. Martin, and I. G. Rigor (1999), Surface air
470 temperature and its variations over the last 150 years, *Rev. Geophys.*, *37*, 173 - 199.
- 471 Kiktev, D., D. M. H. Sexton, L. Alexander, and C. K. Folland (2003), Comparison of
472 modeled and observed trends in indices of daily climate extremes, *J. Clim.*, *16*, 3560 -
473 3571.
- 474 Nakicenovic, N., et al. (2000), Special Report on Emissions Scenarios: A Spe-
475 cial Report of Working Group III of the Intergovernmental Panel on Climate
476 Change, *Cambridge University Press, Cambridge, U.K.*, 599 pp., Available online at:
477 www.grida.no/climate/ipcc/emission/index.htm.

- 478 Sen, P.K., (1968), Estimates of the regression coefficient based on Kendall's tau, *J. Am.*
479 *Stat. Assoc.*, *63*, 1379-1389.
- 480 Sterl A., C. Severijns, W. Hazeleger, G. Burgers, B. van den Hurk, G. J. van Oldenborgh,
481 P. van Velthoven, H. Dijkstra, P. J. van Leeuwen, M. van den Broeke (2008), When
482 can we expect extremely high surface temperatures? *Geophys. Res. Lett.*, *35*, L14703,
483 doi:10.1029/2008GL034071.
- 484 von Storch, H., (1995), Misuses of statistical analysis in climate research, in Analysis of
485 Climate Variability: Application of Statistical Techniques, *edited by H. von Storch and*
486 *A. Navarra*, pp. 11-26, *Springer-Verlag, New York*
- 487 Wang X. L., and V. R. Swail (2001), Changes of Extreme Wave Heights in Northern
488 Hemisphere Oceans and Related Atmospheric Circulation Regimes, *J. Clim.*, *14*, 2204-
489 2221.
- 490 Wheeler B. (2008), SuppDists: Supplementary distributions, *R package version 1.1-2*,
491 <http://www.bobwheeler.com/stat>.
- 492 Yan, Z., P. D. Jones, T.D. Davies, A. Moberg, H. Bengstrom, D. Camuffo, C. Cocheo,
493 M. Maugeri, G. R. Demaree, T. Verhoeve, E. Thoen, M. Barriendos, R. Rodriguez,
494 J. Martin-Vide, and C. Yang (2002), Trends of extreme temperatures in Europe and
495 China based on daily observations, *Clim. Change*, *53*, 355 - 392.
- 496 Zhang X., L. A. Vincent, W.D. Hogg, and A. Niitsoo (2000), Temperature and precipita-
497 tion trends in Canada during the 20th century, *Atmos. Ocean*, *38*, 395-429.
- 498 Zhang X. and F. W. Zwiers (2004), Comment on Applicability of prewhitening to eliminate
499 the influence of serial correlation on the Mann-Kendall test by Sheng Yue and Chun
500 Yuan Wang, *Water Resour. Res.*, *40*, W03805, doi:10.1029/2003WR002073.

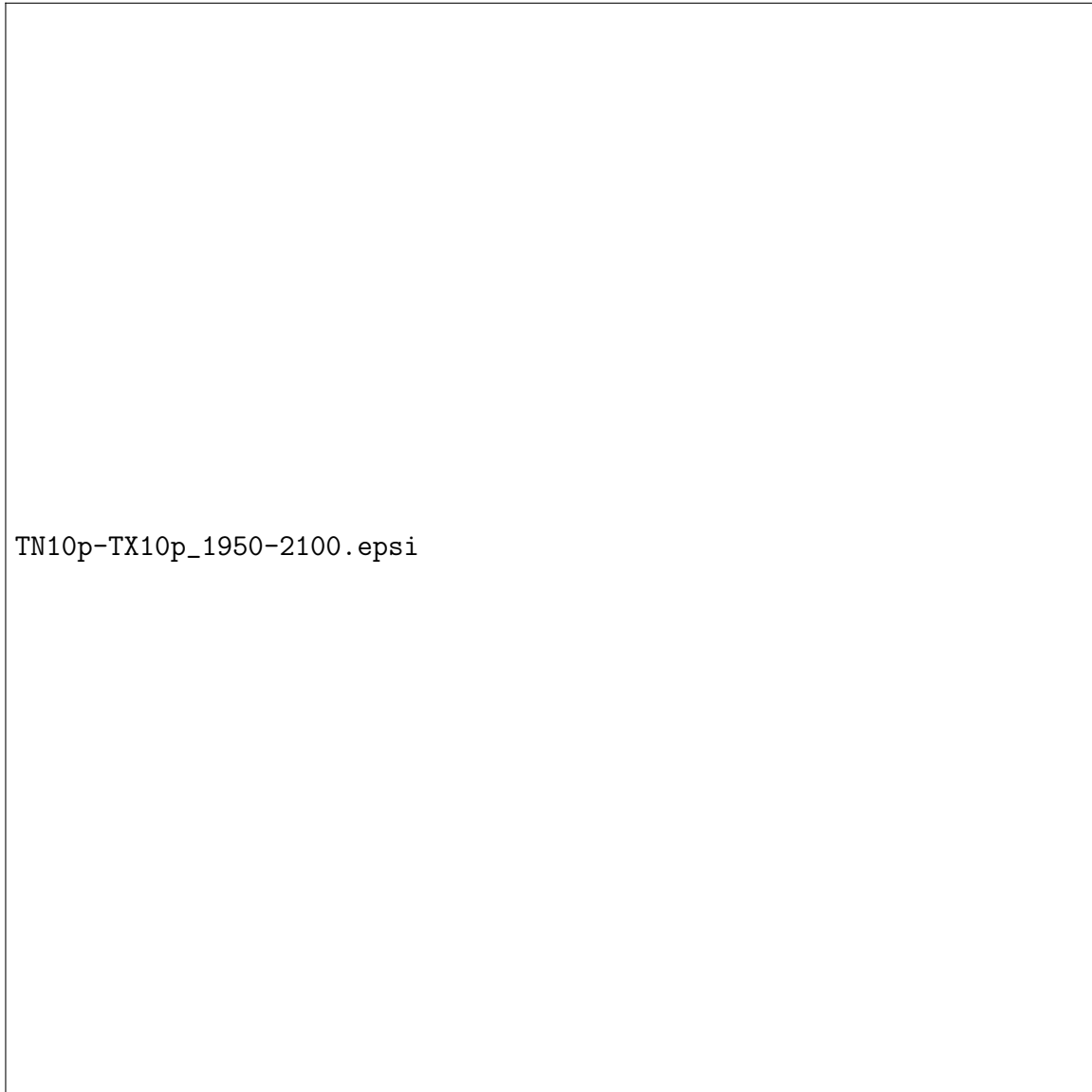


Figure 1. Trend in the numbers of cold nights (TN10p, left) and cold days (TX10p, right) for the periods 1950-2000 (upper), 2001-2050 (middle), and 2051-2100 (lower). The indices are calculated with respect to the respective reference periods. Units are number of days per ten years. In the upper left panel the eight regions defined in Table 2 are indicated.

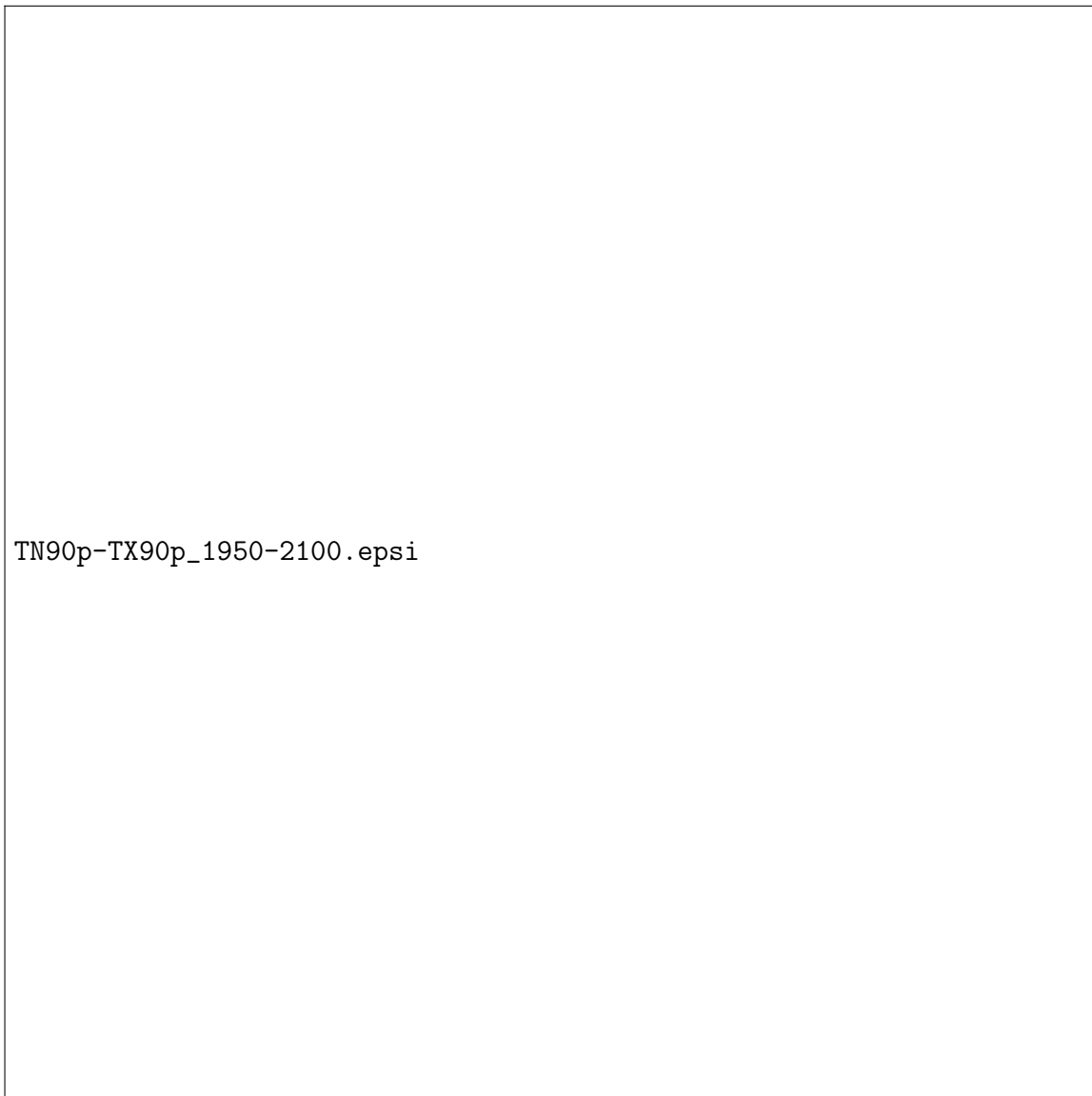


Figure 2. Trend in the numbers of warm nights (TN90p, left) and warm days (TX90p, right) for the periods 1950-2000 (upper), 2001-2050 (middle), and 2051-2100 (lower). The indices are calculated with respect to the respective reference periods. Units are number of days per ten years.

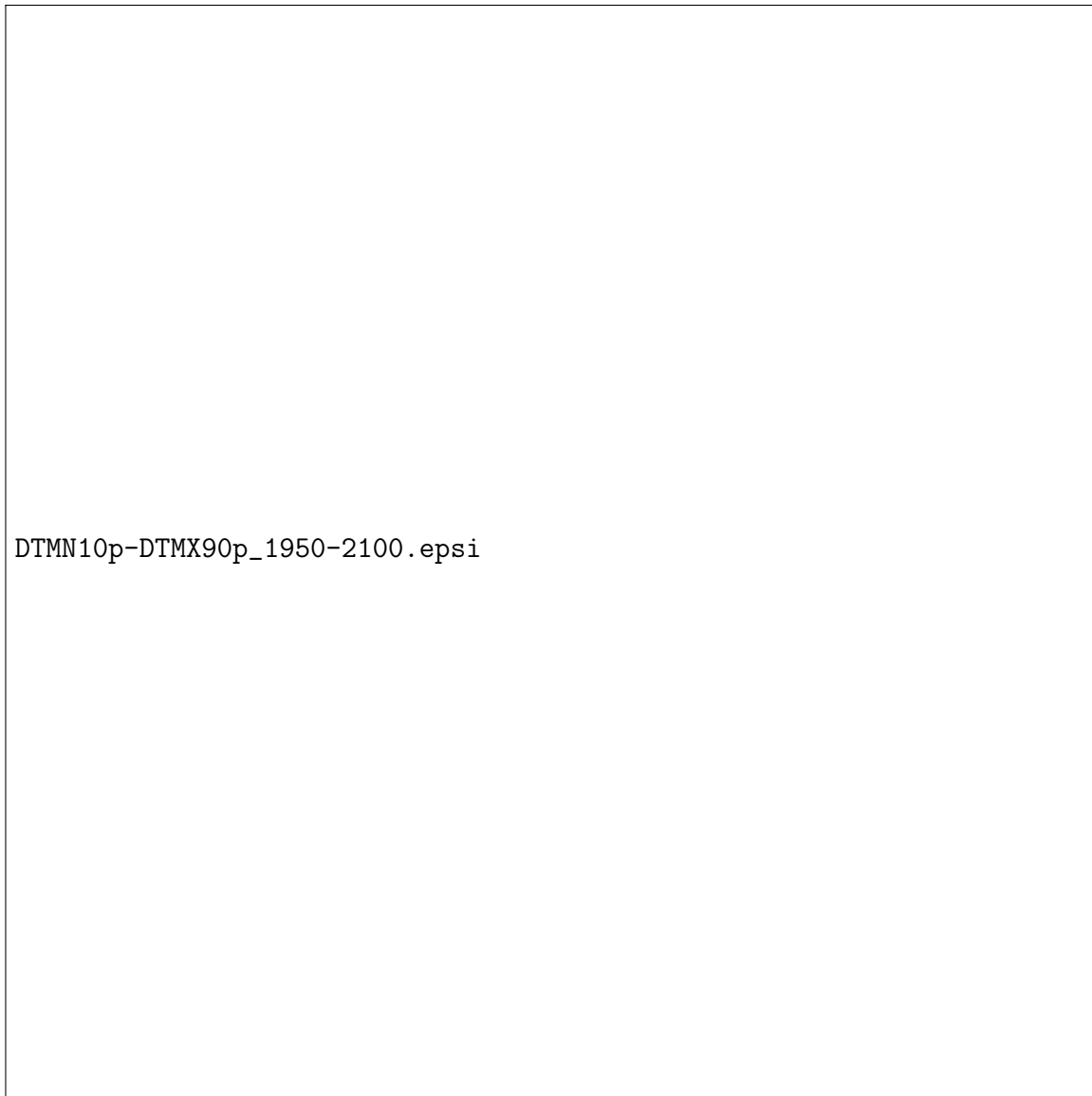


Figure 3. Trend in the intensity of cold nights (ITN10p, left) and warm days (ITX90p, right) for the periods 1950-2000 (upper), 2001-2050 (middle), and 2051-2100 (lower). The indices are calculated with respect to the respective reference periods. Units are degree-days per ten years.

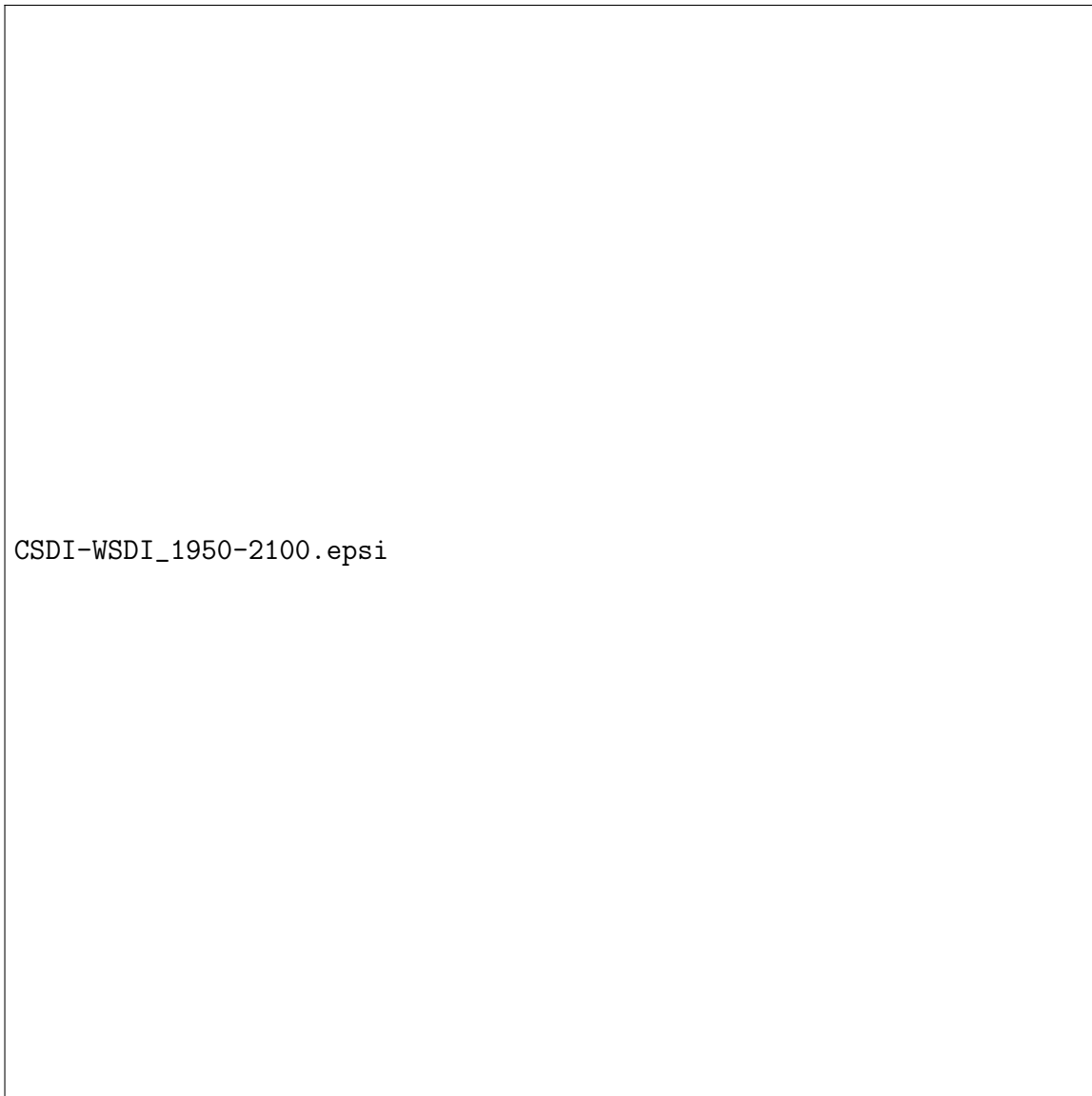


Figure 4. Trend in the duration of cold spells (CSDI, left) and warm spells (WSDI, right) for the periods 1950-2000 (upper), 2001-2050 (middle), and 2051-2100 (lower). The indices are calculated with respect to the respective reference periods. Units are days per ten years.

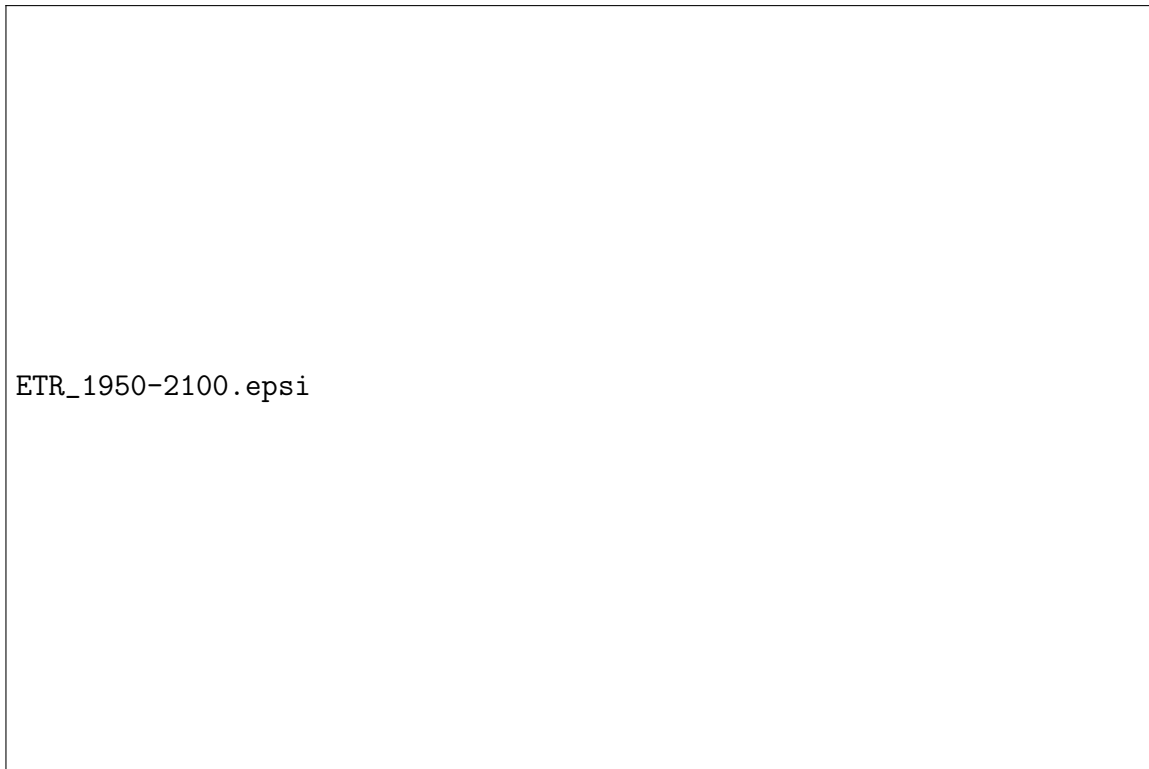


Figure 5. Trend in the yearly temperature range (ETR) for the periods 1950-2000 (upper left), 2001-2050 (upper right), and 2051-2100 (lower left). The indices are calculated with respect to the respective reference periods. Units are Kelvin per ten years.

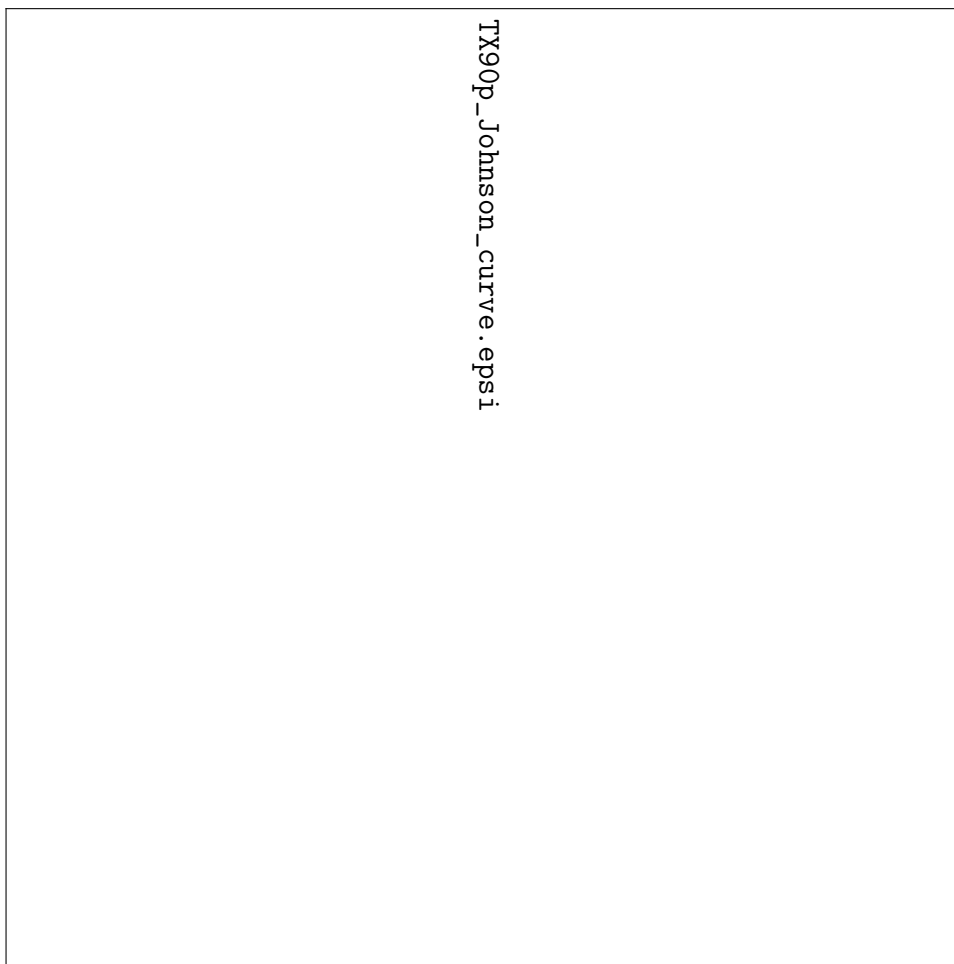


Figure 6. Johnson’s PDF of TX90p for the six 25-year periods (black: 1950-1975, grey: 1976-2000, cyan: 2001-2025, blue: 2026-2050, orange: 2051-2075, and red: 2076-2100). Number of events for each PDF N=425.

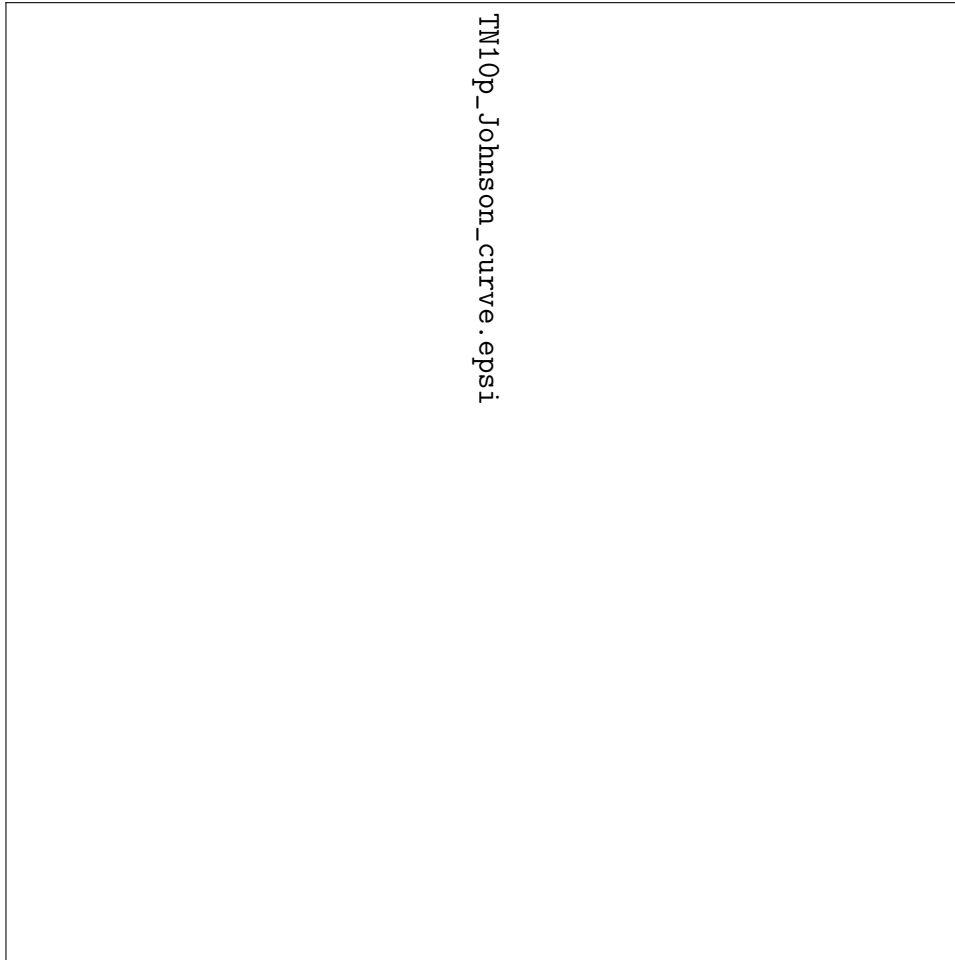


Figure 7. Johnson's PDF of TN10p-ft for the six 25-year periods (black: 1950-1975, grey: 1976-2000, cyan: 2001-2025, blue: 2026-2050, orange: 2051-2075, and red: 2076-2100). Number of events for each PDF N=425.

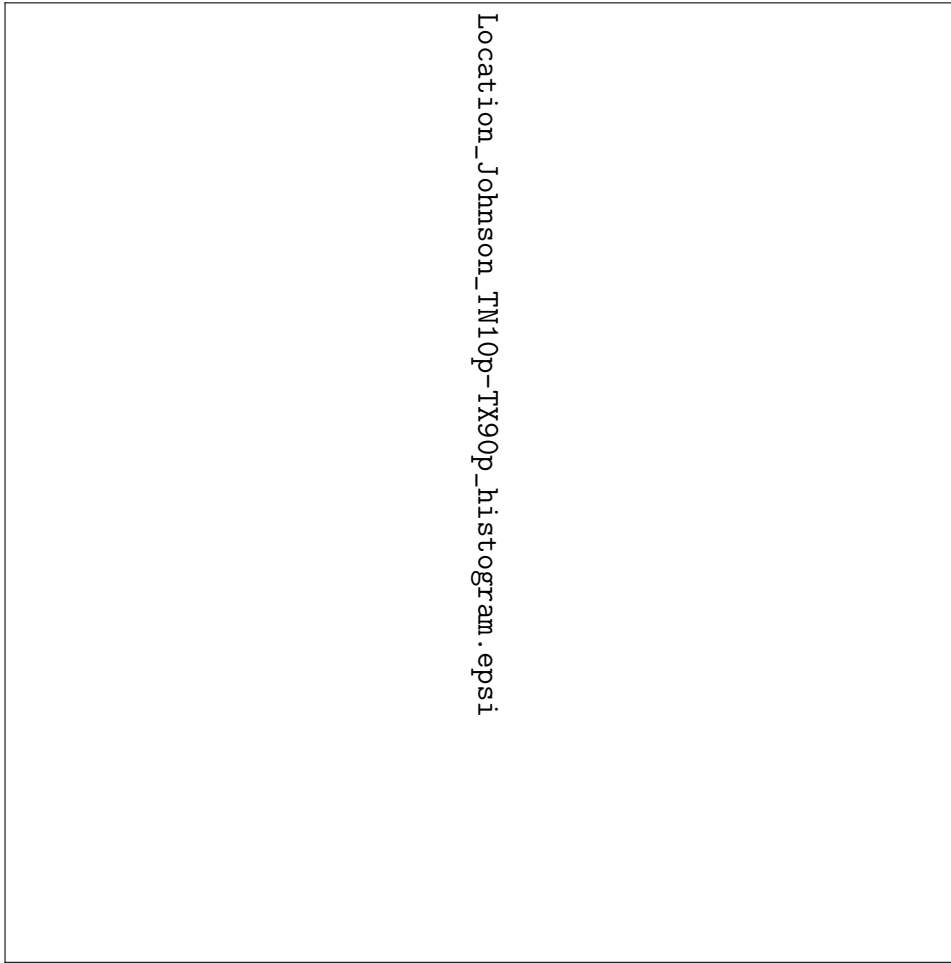


Figure 8. Development over time of the location parameters of TX90p (black circles) and TN10p-ft (grey crosses) in the eight regions of Table 2. The red symbols denote the index ΔE_i as defined in (11) for TX90p. The periods are indicated by the numbers on the x-axis (1: 1951-1975, 2: 1976-2000, ..., 6: 2076-2100). The index values on the y-axis are expressed in percent of days in a year and represent the change between the location parameter for the given 25-year period and that of the first period (1951-1975). Panel i) shows the difference of the location parameters between the last and the first period, respectively (black: TX90p, grey: TN10p-ft).

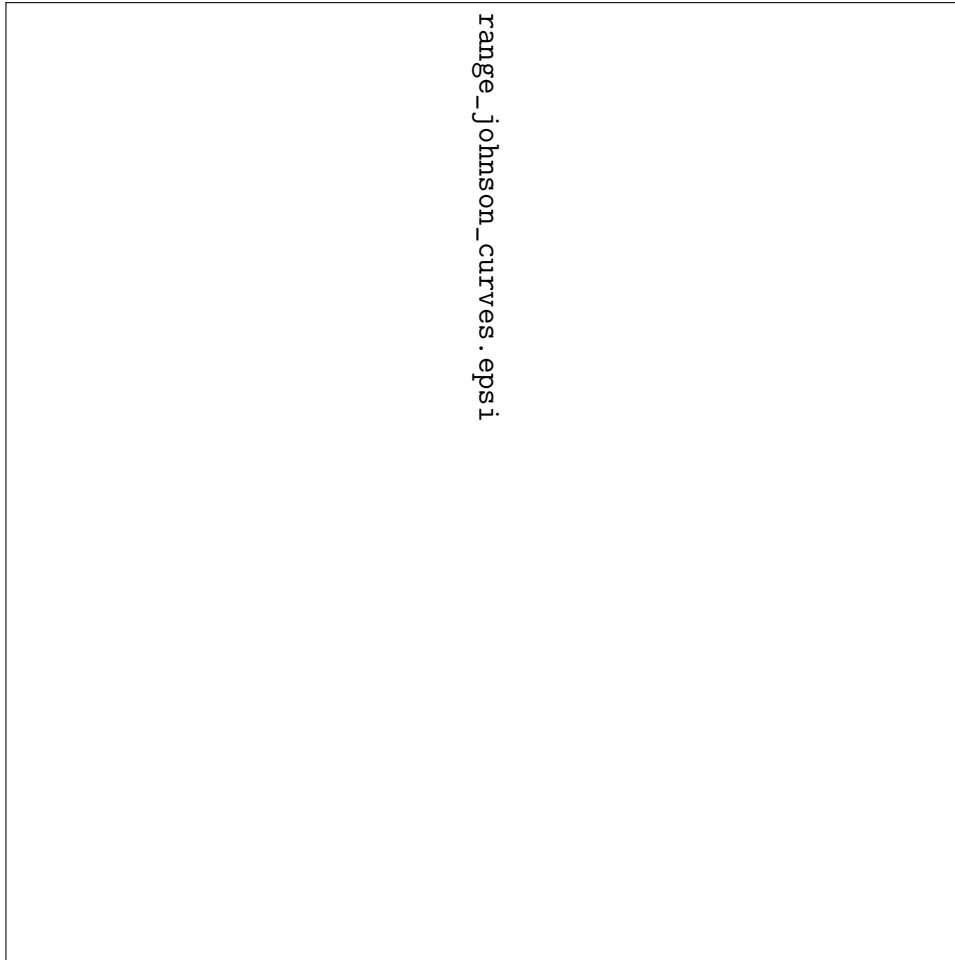


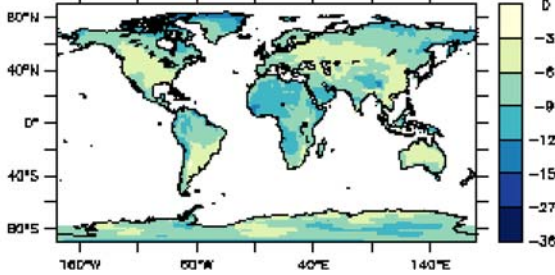
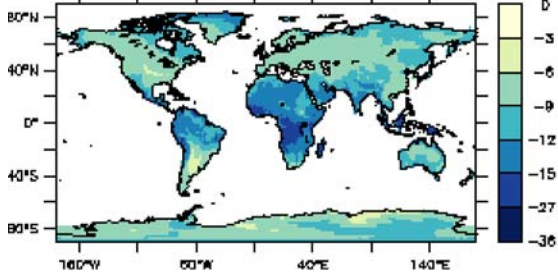
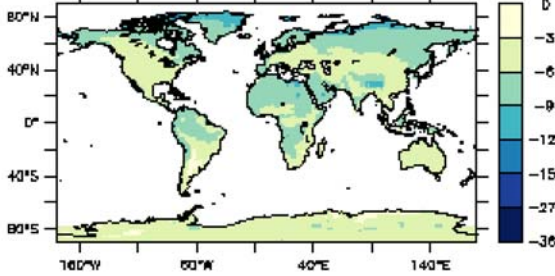
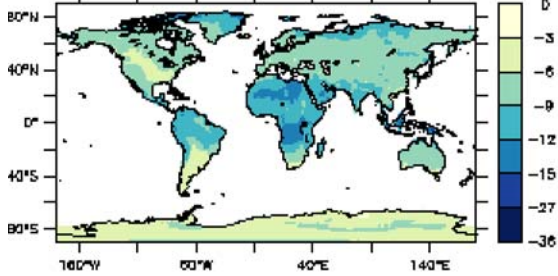
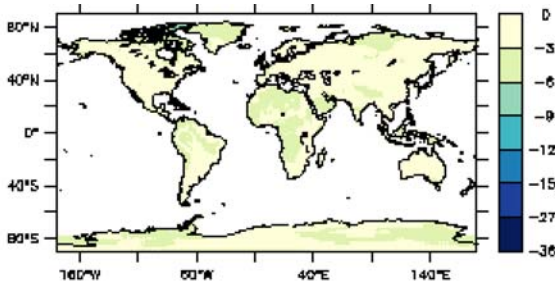
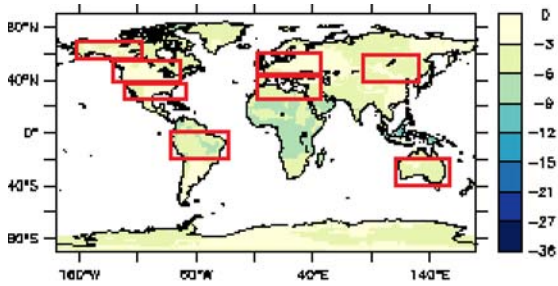
Figure 9. Johnson’s PDF of ETR for the six 25-year periods (black: 1950-1975, grey: 1976-2000, cyan: 2001-2025, blue: 2026-2050, orange: 2051-2075, and red: 2076-2100). Number of events for each PDF $N=425$.

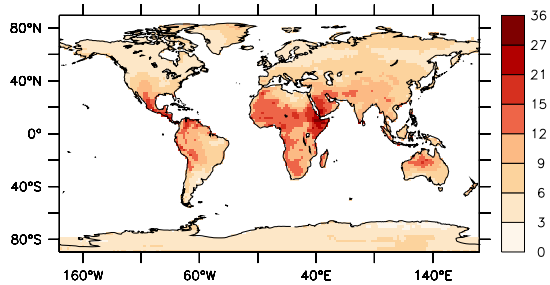
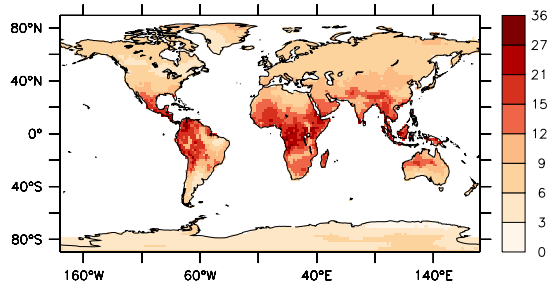
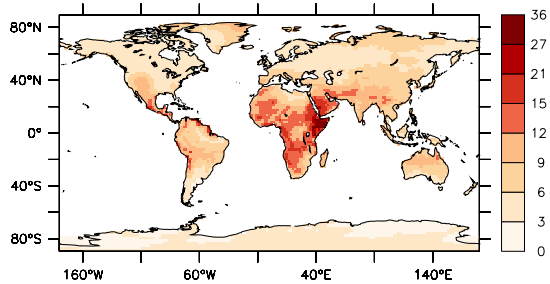
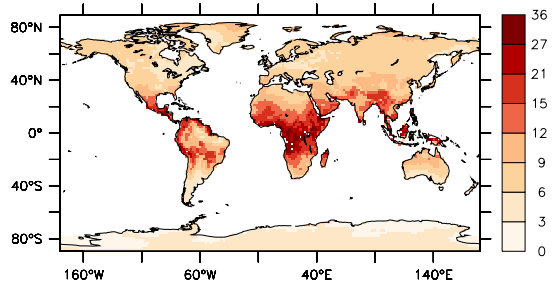
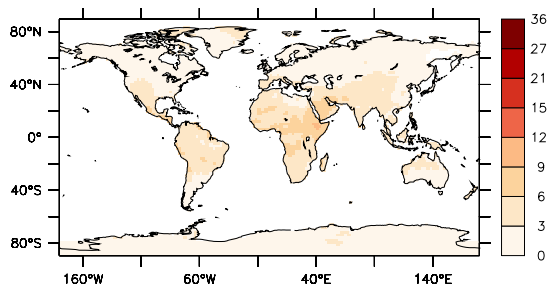
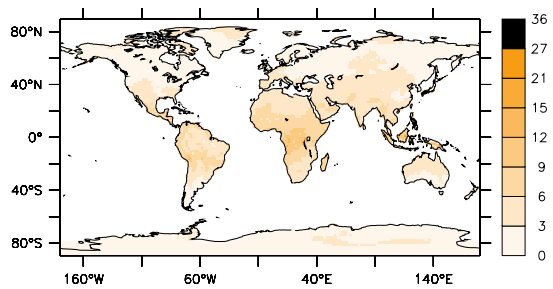
Index	Definition	Unit
TX90p	Warm days: percent (or numbers) of days per month with daily maximum temperature over the 90th percentile for the 1961-1990 reference period.	days
TN90p	Warm nights: As TX90p, but using minimum daily temperature.	days
TX10p	Cold days: percent (or numbers) of days per month with daily maximum temperature below the 10th percentile for the 1961-1990 reference period.	days
TN10p	Cold nights: As TX10p, but using minimum daily temperature.	days
TN10p-ft	Percent (or numbers) of days by month with minimum daily temperature over the 10th percentile for the 2061-2090 reference period. Applied to whole 1950-2100 period.	days
ITX90p	Intensity of warm spells: Degree-days above 90% threshold.	degree-days
ITN10p	Intensity of cold spells: Degree-days below 10% threshold.	degree-days
WSDI	Warm spell duration: Maximum period with more than 5 consecutive days with maximum temperature above the 90th percentile for the 1961-1990 reference period.	days
CSDI	Cold spell duration: Maximum period with more than 5 consecutive days with minimum temperature below the 10th percentile for the 1961-1990 reference period.	days
ETR	Intra-annual extreme temperature range: difference between the highest temperature observation for any given calendar year and the lowest temperature reading of the same calendar year.	days

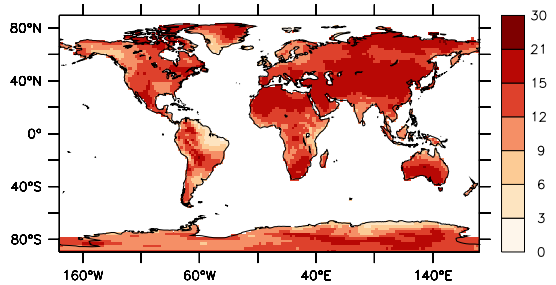
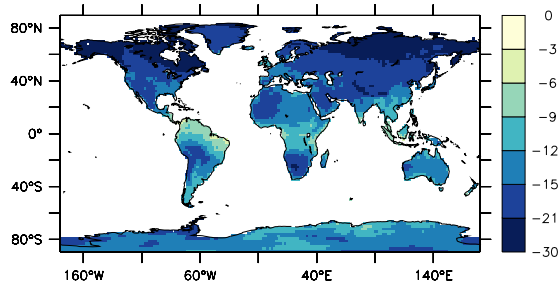
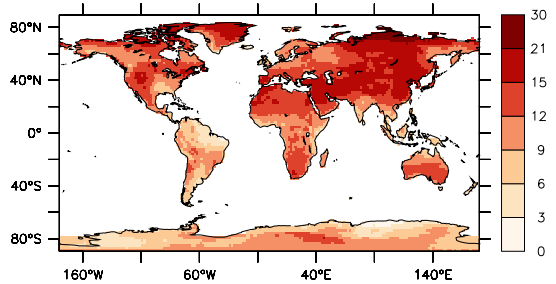
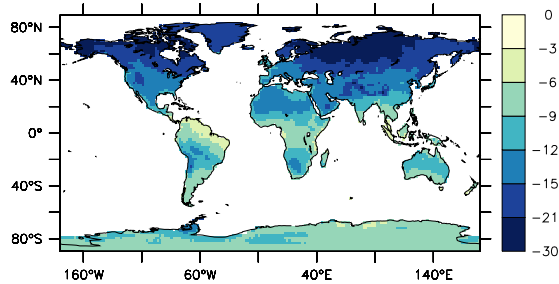
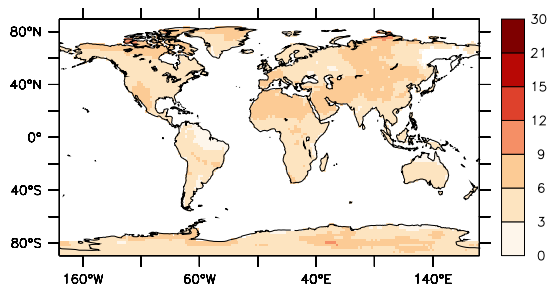
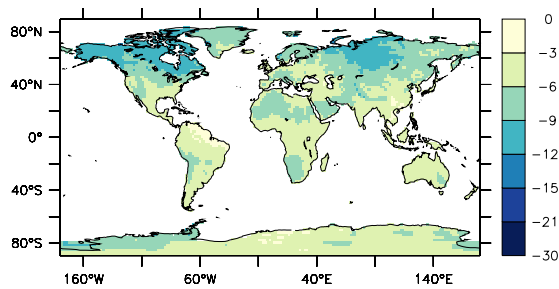
Table 1. Definition of indices.

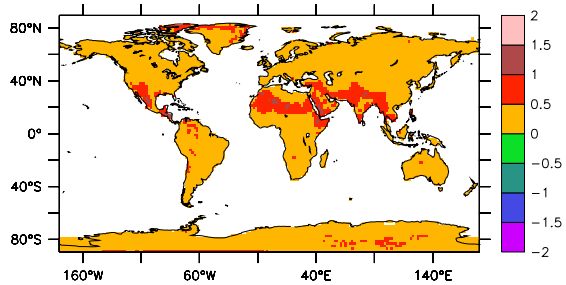
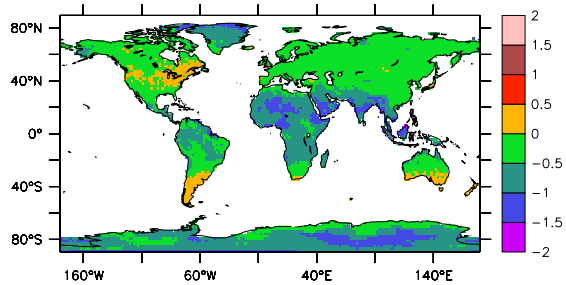
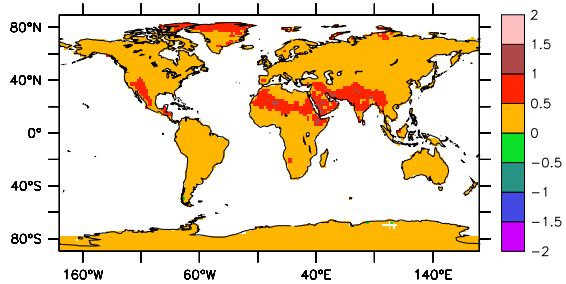
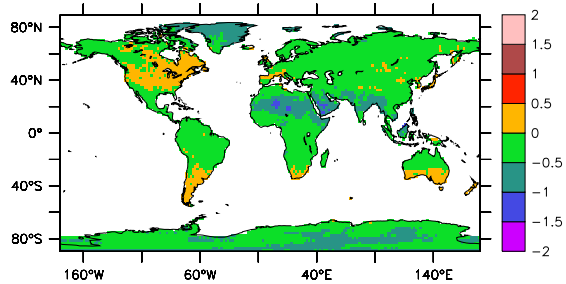
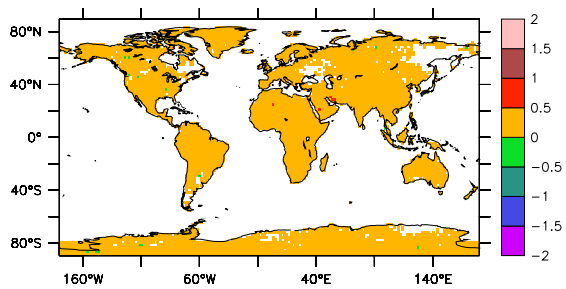
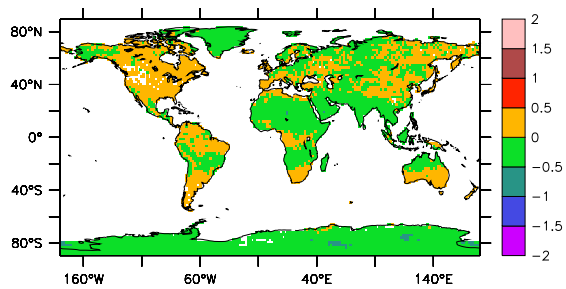
	Alaska	Canada	USA	Europe
Latitude	58-70°N	38-58°N	27-38°N	45-60°N
Longitude	165-105°W	130-70°W	120-65°W	15°W-45°E
	Med-Countries	Northern South America	Australia	Russia
Latitude	27-45°N	0-21°S	20-40°S	40-60°N
Longitude	15°W-45°E	90-30°W	110-160°E	80-120°E

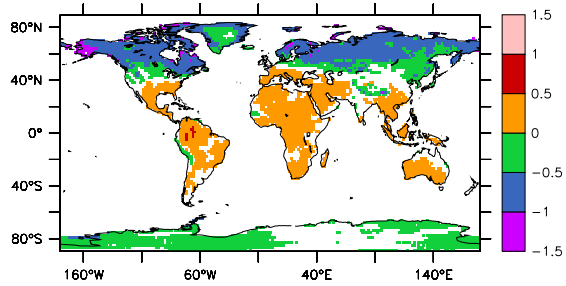
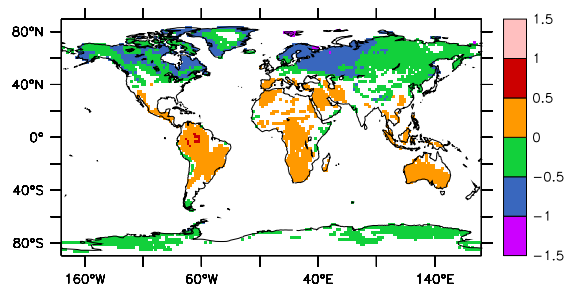
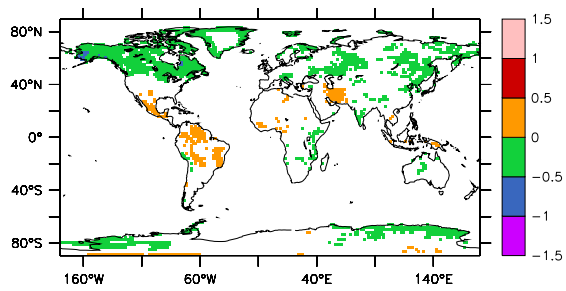
Table 2. Definition of regions used to calculate the PDFs.



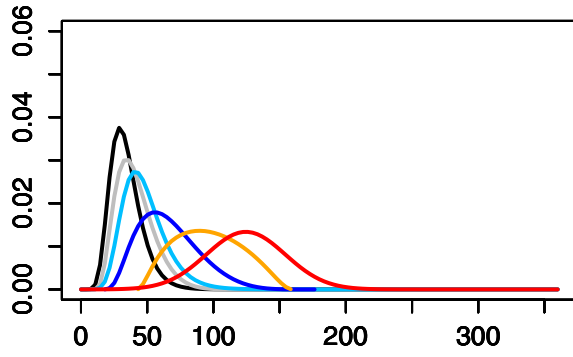




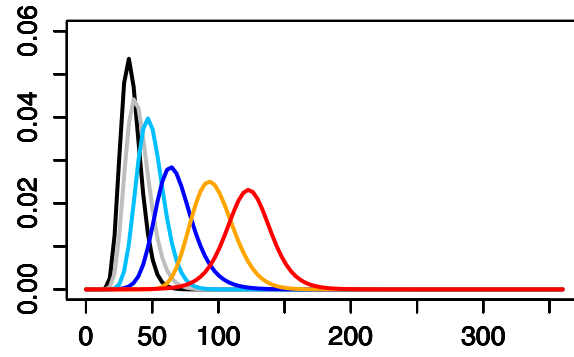




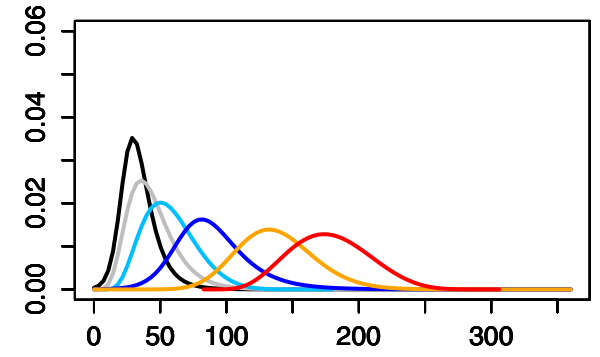
a) Alaska



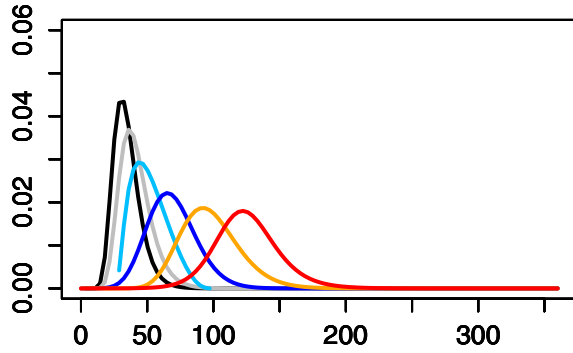
b) Canada



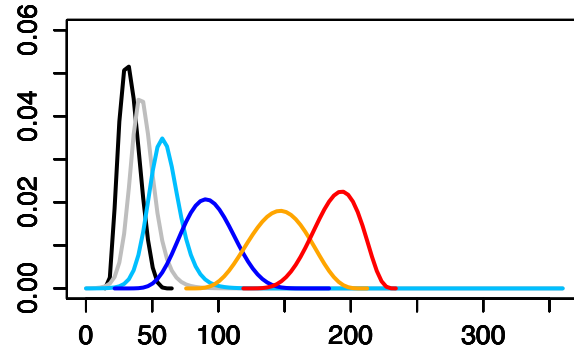
c) USA



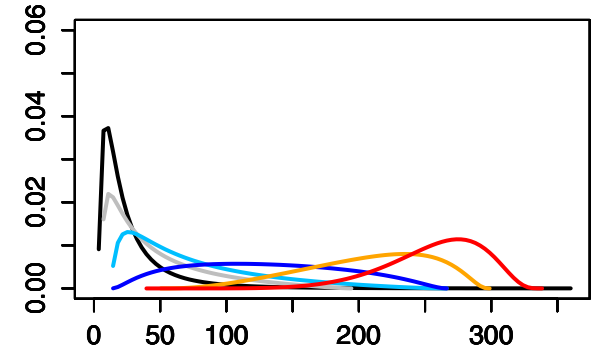
d) Europe



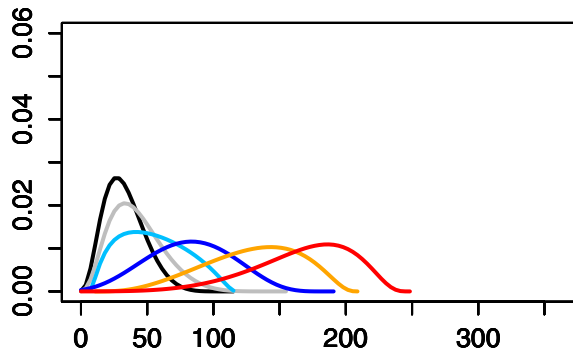
e) Med-Countries



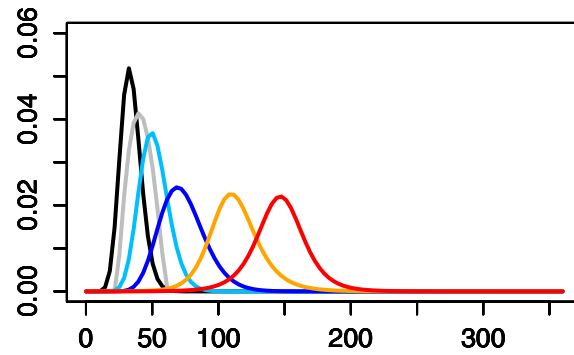
f) N-S America



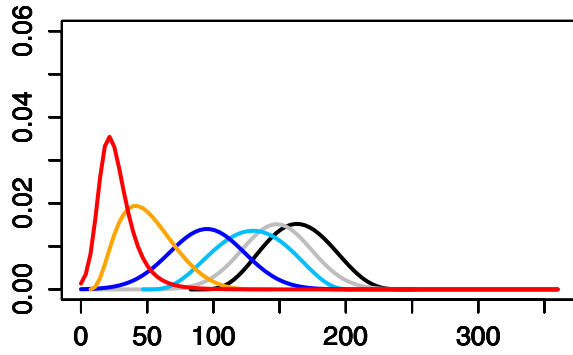
g) Australia



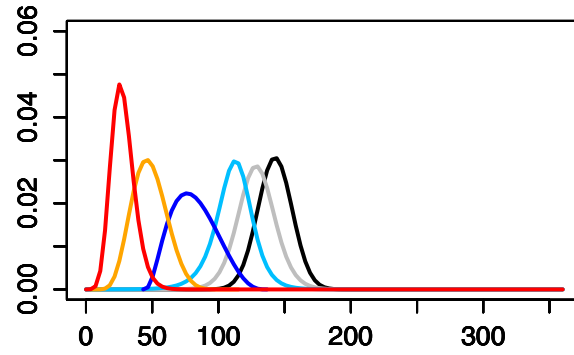
h) Russia



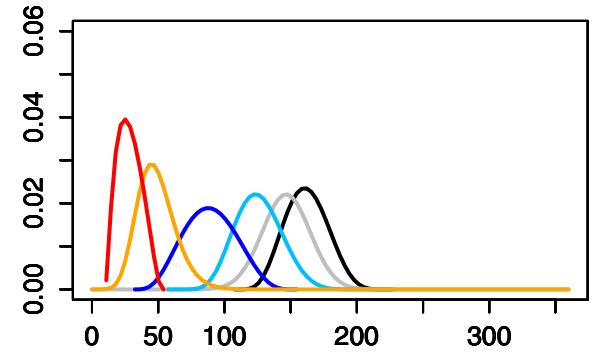
a) Alaska



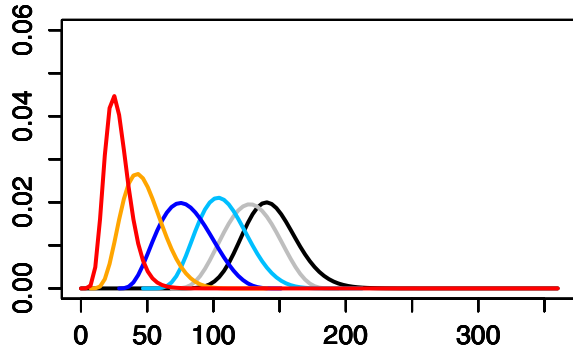
b) Canada



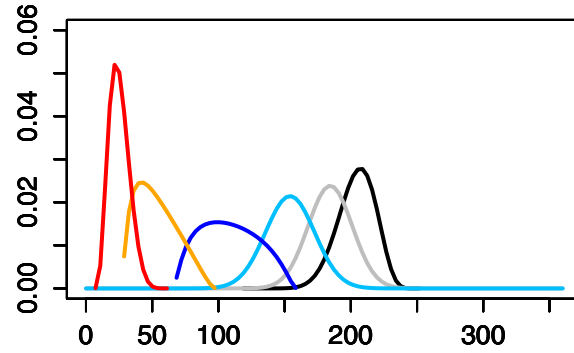
c) USA



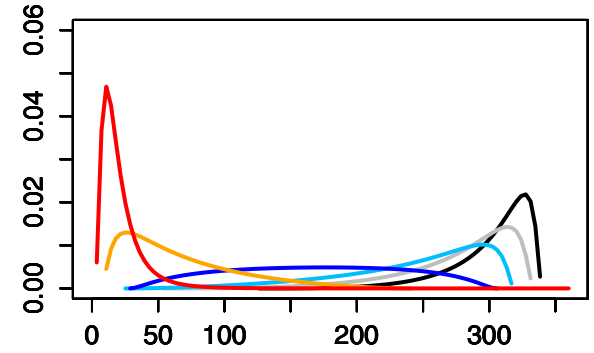
d) Europe



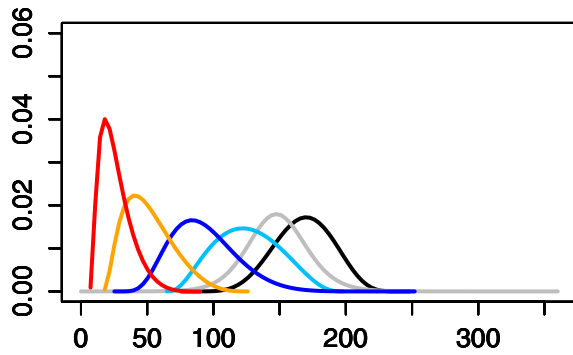
e) Med-Countries



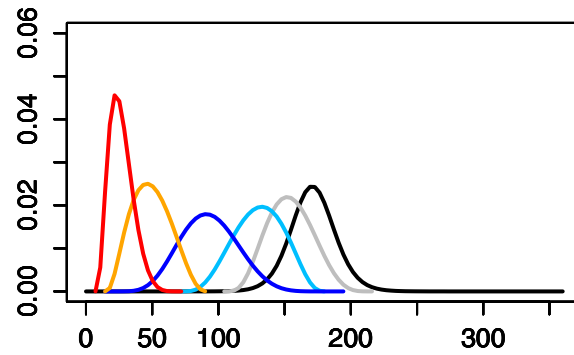
f) N-S America



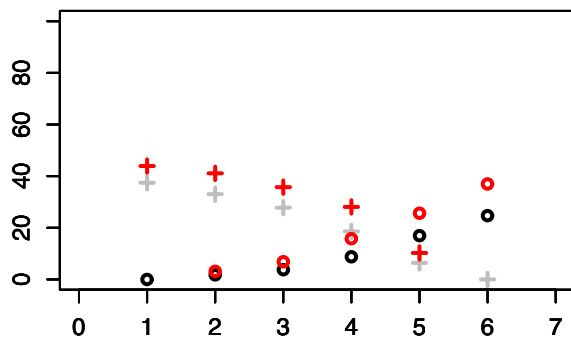
g) Australia



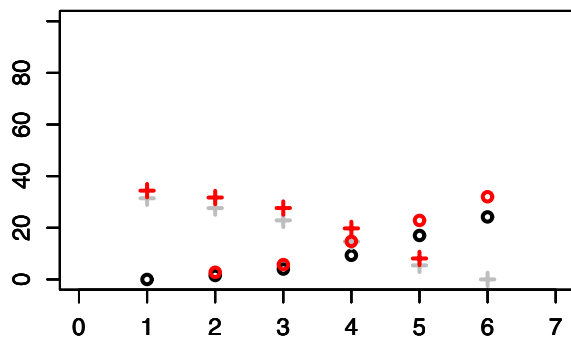
h) Russia



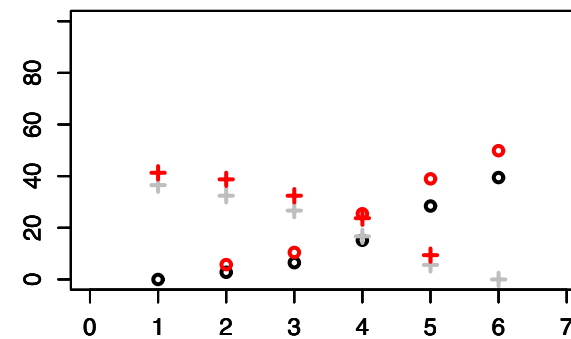
a) Alaska



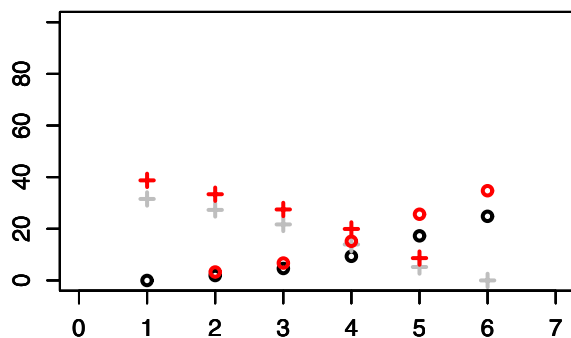
b) Canada



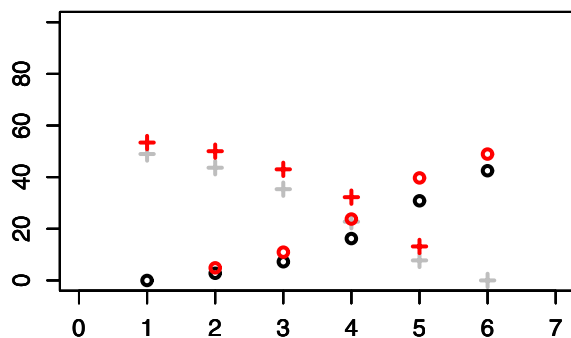
c) USA



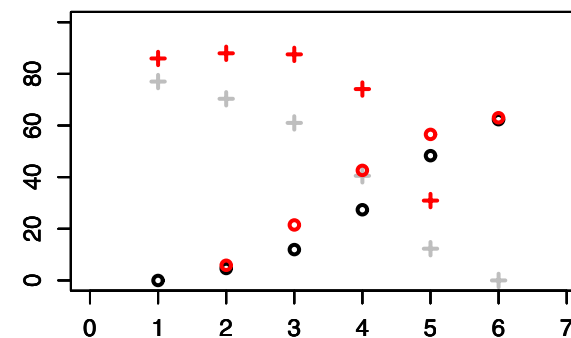
d) Europe



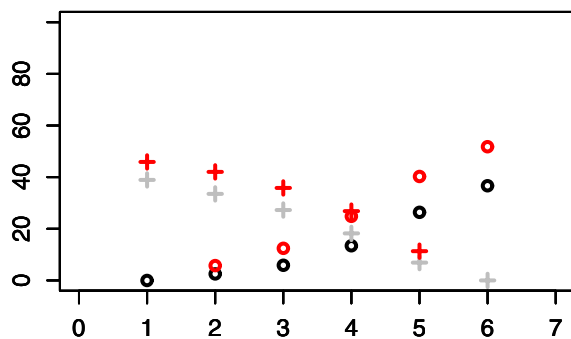
e) Med-Countries



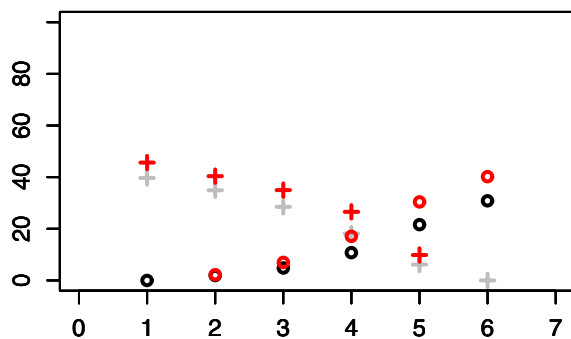
f) N-S America



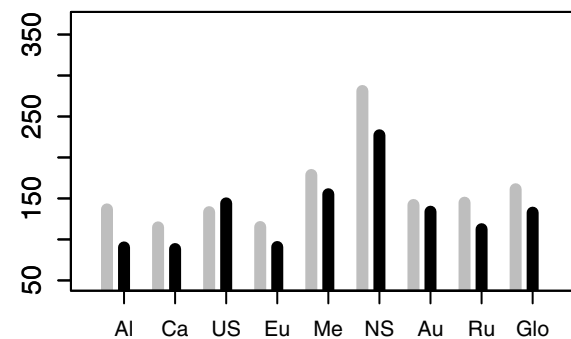
g) Australia



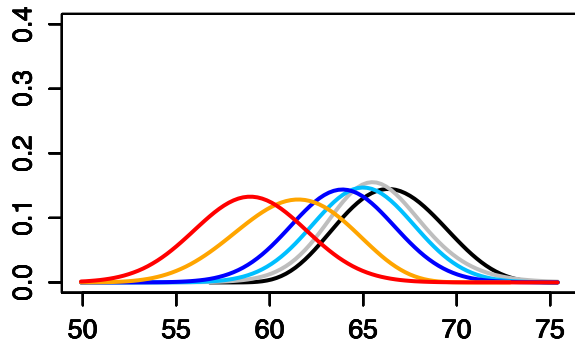
h) Russia



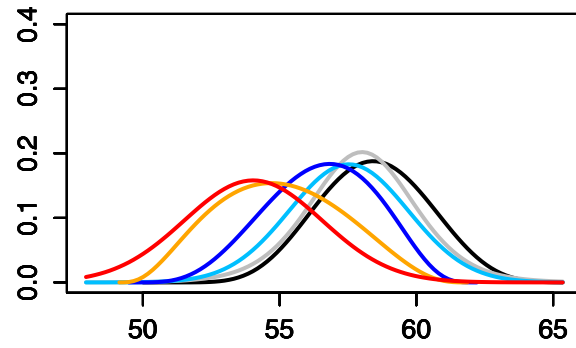
i)



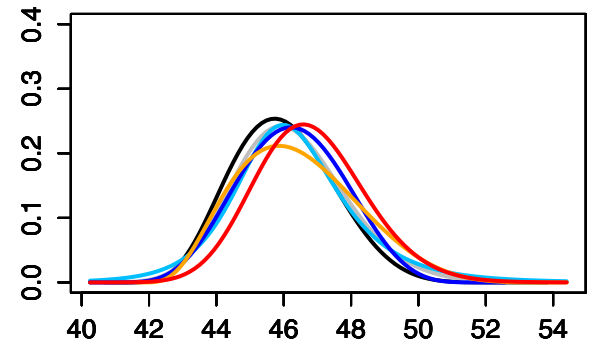
a) Alaska



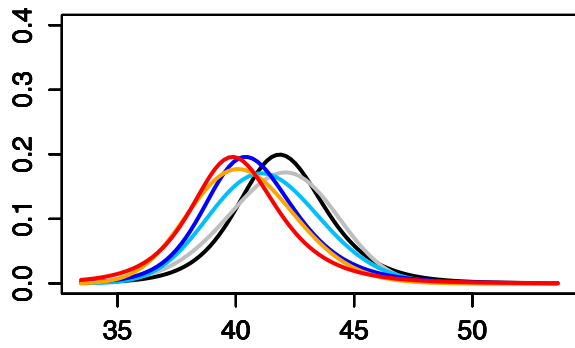
b) Canada



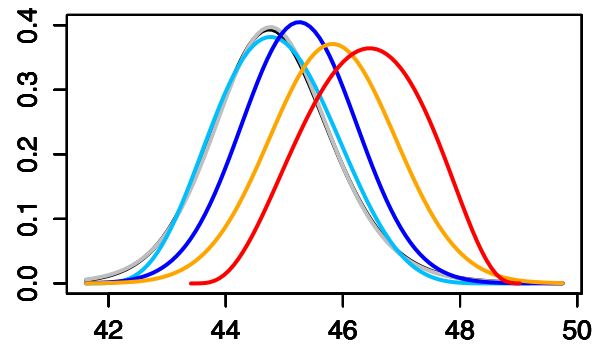
c) USA



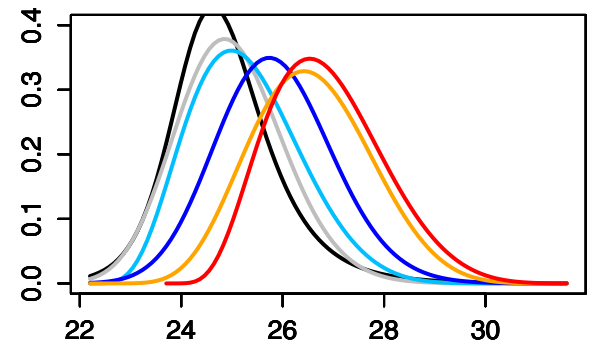
d) Europe



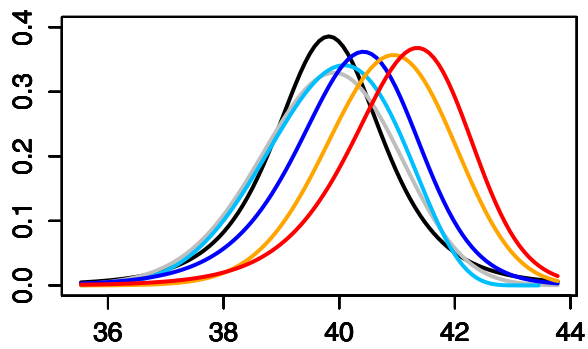
e) Med-Countries



f) N-S America



g) Australia



h) Russia

